Durham E-Theses

The charge excess and momentum spectrum of cosmic ray muons in the vertical direction

Aurela, A. W.

How to cite:

Aurela, A. W. (1965) *The charge excess and momentum spectrum of cosmic ray muons in the vertical direction*, Durham theses, Durham University. Available at Durham E-Theses Online: http://etheses.dur.ac.uk/10511/

Use policy

The full-text may be used and/or reproduced, and given to third parties in any format or medium, without prior permission or charge, for personal research or study, educational, or not-for-profit purposes provided that:

- a full bibliographic reference is made to the original source
- a link is made to the metadata record in Durham E-Theses
- the full-text is not changed in any way

The full-text must not be sold in any format or medium without the formal permission of the copyright holders.

Please consult the full Durham E-Theses policy for further details.

The Charge Excess and Momentum Spectrum

of Cosmic Ray Muons in the

Vertical Direction

by

A. M. Aurela, M.A., Phil. Lic.

A Thesis submitted to the

University of Durham for the

Degree of Doctor of Philosophy

November, 1965.

CONTENTS

ABSTRACT

The charge excess and momentum spectrum of cosmic ray muons have been measured at 60 m above sea-level by means of the "Vertical Durham Spectrograph" which had been modified in many respects (e.g. by the addition of a solid iron plug of thickness 45 cm) and re-aligned and calibrated. The effect of the multiple scattering in the magnet is found to be the most serious limitation of the instrument and methods of coping with it are investigated, among others a new statistical method.

The values obtained for the charge ratio are 1.240 ± 0.036 at 12 GeV/c, 1.262 ± 0.031 at 23 GeV/c, 1.279 ± 0.038 at 31 GeV/c, 1.208 ± 0.069 at 47 GeV/c, 1.269 ± 0.085 at 66 GeV/c, and 1.324 ± 0.111 at 102 GeV/c. These results have been combined with the results of previous workers. The best estimates thus obtained are compared with the theoretical expectations calculated by MacKeown et al. (1965a). The expectations are calculated for an empirical model of nuclear interactions including kaons, for the isobar model (Peters, 1963; Yash Pal, 1963), and for the peripheral collision model (Narayan, 1964; Crossland and Fowler, 1965), including the empirical low-energy pionization in the two latter models. A qualitative agreement is found between the experiments and theory in each case but quantitative conclusions

cannot be drawn because of the statistical errors of the experimental results and because of uncertainty in the parameters of the models.

The momentum spectrum observed agrees well with the spectrum given by Osborne et al. (1964) within the accuracy of the instrument. The underground muon spectrum observed by Vernov et al. (1965) and the spectrum of primary nuclei measured by the satellite Proton I (Grigorov et al., 1965; Vernov, 1965) disagree with the present results.

PREFACE

This thesis describes the final experiment of a long series performed with the "Vertical Cosmic Ray Spectrograph" in the University of Durham under the general supervision of Professor A. W. Wolfendale.

The present work was started in October 1962. During the preparation of the experiment, Mr. K. Gijsbers was mainly responsible for the work, until he left the country in June 1964. Dr. Y. Kamiya also worked on this project until May 1964. The contributions of these two workers are acknowledged at the appropriate points in the thesis. The author joined the experiment in October 1963 and had the main responsibility for the work during the actual experiment. Drs. G. Brooke and K. M. Pathak collaborated in the experiment. The methodological corrections to the data (Chapter 4) and the subsequent comparisons and interpretation were the sole responsibility of the author.

CHAPTER 1

INTRODUCTION

Research into the energy spectrum of cosmic ray muons had its origin in the cloud chamber experiments of the 1930's, actually before muons had been distinguished from protons and electrons. As a side-result, these experiments also revealed a difference in abundance between positive and negative muons, the so-called positive excess or charge excess. Rossi (1948) collected the results of the early experiments and gave a momentum spectrum in the region of 1 GeV/c in terms of absolute intensities. Later, the measurements of the muon spectrum and the charge excess were extended to higher momenta by various methods. The theoretical interpretation of the results gave fundamental information on the high-energy neclear interactions involved in the propagation of cosmic-ray particles through the atmosphere. Apart from its role in nuclear physics, muon research also took a rather central position in cosmic ray phenomenology proper. The development of research on the charge excess and momentum spectrum of muons prior to 1960 was reviewed by Fowler and Wolfendale (1961).

For the needs of this thesis it suffices to review only the status of the research at about the time of the preparations of the present experiment. According to the rapporteur paper given by Rochester (1963), at the International Conference on Cosmic Rays in Jaipur, the vertical muon spectrum was known at that time with an accuracy of 5-10% for momenta up to 100 GeV/c and with less accuracy up to 1000 GeV/c. The main source of information below 1000 GeV/c was the measurements with cosmic ray spectrographs (e.g. Hayman and Wolfendale, 1962). Between 1000 and 5000 GcV/c, the spectrum was deduced indirectly by three different methods. Firstly, the spectrum was derived from the gamma-ray cascades observed in nuclear emulsions exposed in the atmosphere on the assumption that the muons came only from pion parents (Duthie et al., 1962). Secondly the momentum spectrum was deduced from the size spectrum of the muon bursts recorded in ionization chambers (Krasilnikov, 1963; Kitamura and Takahashi, 1963; see also Higashi et al., 1964). These two methods gave consistent results at 1000 GeV/c but the burst spectrum gave progressively higher intensities at greater momenta; at 5000 GeV/c it was higher by a factor 4. It was thought that the first method gave too low

values because some of the parent particles should be kaons. Furthermore, according to the experiments of the Japanese and Brazilian Emulsion Groups (1963) there was also a marked error in the slope of the gamma spectrum of Duthie et al. On the other hand, the second method was believed to lead to an overestimate because of the effect of fluctuations and nuclear interactions in the walls of the ionization chambers. Additional controversy was caused by the momentum spectrum measured at 40 m w.e. underground by Dmitriev and Khristiansen (1963) by a burst experiment. At high momenta their results were much higher than those from other burst experiments, the discrepancy being a factor of 10 at 8000 GeV/c. The third method for the determination of the sea-level muon spectrum was provided by the analyses of underground muon intensities (Ramana Murthy, 1963; see also Miyake et al., 1964). The corresponding spectrum lay between those obtained as described above but was nevertheless considered unsure because of the many assumptions involved in such analyses. In general, the uncertainty in the momentum spectrum was more methodological than statistical.

The excess of the positive muons has been represented quantitatively by the so-called charge ratio R or by the

relative charge excess η. These quantities are defined by the following equations:

$$R(p) = i_+(p)/i_-(p) \qquad 1.1$$

$$\eta(p) = (i_+ - i_-)/(i_+ + i_-) \qquad 1.2$$

where $i_+(p)$, and $i_-(p)$ are the differential momentum spectra of the positive and negative muons, respectively. (In the case of the relative charge excess, another definition has also been used; see e.g. Fowler and Wolfendale, 1961). Until the time of the Jaipur Conference, the measurements of the charge excess had been extended up to about 500 GeV/c, although with very poor statistics. The only source of information was the spectrograph measurements. The charge ratio had been found to remain roughly constant at about 1.25 with an indication of a slight minimum between 20 and 50 GeV/c and a tendency to rise above the average between 50 and 500 GeV/c (MacKeown et al., 1963), although it should be pointed out that the measurements made showed a remarkable degree of dispersion. The variation of R with momentum was given more emphasis than the statistics alone allowed, because a change in the production mechanism at high momenta could introduce some variation.

On the theoretical side, the principal features of the propagation of cosmic rays through the atmosphere could be

accounted for with the basic assumptions of isobars and a little pionisation (Peters, 1963; Yash Pal, 1963). A qualitative agreement between theory and experiment was obtained for the variation of muon charge excess with momentum, and the abundance ratios of neutrons to protons, pions to protons, and kaons to pions. However, many of the features of cosmic rays in the atmosphere could equally well be accounted for by other reasonable models (Grigorov et al., 1963; Grigorov and Shestoperov, 1963; MacKeown et al., 1963; Wolfendale, 1963). The conclusion was therefore that many cosmic ray phenomena are relatively insensitive to the model especially in view of the fact that there were many adjustable parameters.

The present experiment was planned to improve the accuracy of the experimental data on the charge excess at high momenta by means of the "Vertical Cosmic Ray Spectrograph" of the University of Durham. As the same basic data could be used for the determination of the momentum spectrum, this objective was also included into the project. This experiment resembles the earlier work of Hayman and Wolfendale (1962) carried out with the Vertical Spectrograph, but several modifications have been made to it since then, the most important change being the installation of an iron plug in the electro - magnet (Palmer, 1964). Hence an essentially new instrument

was used in this case and the results are quite independent of the earlier measurement. Great emphasis was laid during the present experiment on high precision in the measurement of the characteristics of the spectrograph, such as the geometrical constants (section 3.1) and the magnetic field (section 3.2), and in the methodological corrections (Chapter 4).

In connection with the methodological corrections of the experiment (section 4.2) a statistical problem was encountered which seemed to be important not only in the present work but in all experiments using spectrographs with solid iron magnets (in fact, in all indirect determinations of unknown distribution functions). This problem has been studied in detail as far as was reasonable within the scope of the work. Apart from this, the theoretical part of the work consists of an interpretation of the experimental results (Chapter 6).

The present work was linked with another project going on in Durham, namely the measurement of the charge excess in a nearly horizontal direction (MacKeown et al., 1963). Since the decay probabilities of pions and kaons should vary in different ways with the zenith angle, a difference might exist between the results obtained in the vertical and horizontal direction, reflecting the portion of kaons in the meson production.

CHAPTER 2

THE EXPERIMENTAL EQUIPMENT

2.1 General features of the spectrograph

The original Durham cosmic ray spectrograph was described
by Brooke et al. (1962) and by Jones et al. (1962). Later on,
the spectrograph was essentially modified by Hayman and
Wolfendale (1962) and again by Palmer (1964) and his colla-
borators. In this work, some further modifications were made
as will be accounted for at the appropriate points in the
sequel.

The spectrograph consisted basically of an electromagnet
to cause a deflection of incoming charged particles and a
detector system for the purpose of measuring the deflection
(Fig. 2.1). In the present experiment, the effective part
of the magnet was an iron plug of dimensions 45 cm x 45 cm x
40 cm, the field being in the geographic east-west direction.
The detector system involved four Geiger counter trays for
the initial detection of a particle and four flashtube arrays
for accurate location of the particle trajectory.

The principle of the use of the spectrograph was as
follows: The statistical frequency distribution of particle
deflections was observed, taking into account the sign of the
deflection. The momentum spectrum was then calculated according
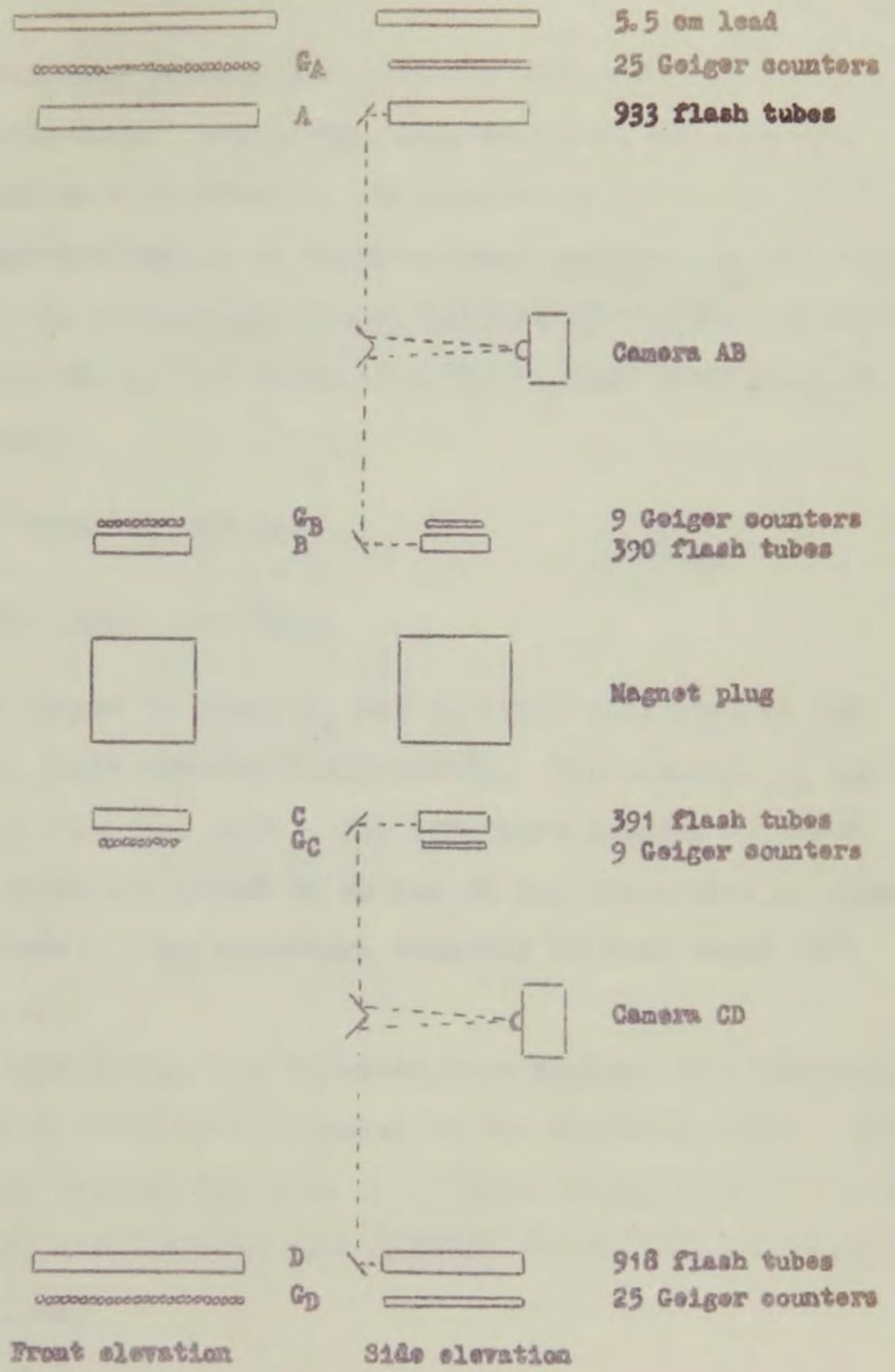
Fig. 2.1 The basic elements of the spectrograph.

to the relation between the particle momentum and the magnetic deflection. Similarly, the charge excess could be determined as a function of the momentum. In the calculations, account had to be taken of the variation of the acceptance of the spectrograph with the particle deflection and a correction was needed because of the Coulomb scattering in the magnet.

2.2 The detector system

2.2.1 The Geiger counters

The Geiger counters G_A and G_D (Fig. 2.1) were of the type G.60 (20th Century Electronics). The counters G_B and G_C were of the type G.26. The effective lengths of these counter types are about 60 cm and 25 cm, respectively (Brooke et al., 1962). The effective diameter of both types is 3.4 ± 0.1 cm.

At each level, the counters were mounted in a horizontal plane, with their axes parallel to the magnetic field. The separation between the axes of adjacent counters was 3.8 cm. In a tray, the counters were mounted to the correct positions within ± 1 mm.

2.2.2 The flash tubes

The flash tubes were glass tubes which had been painted
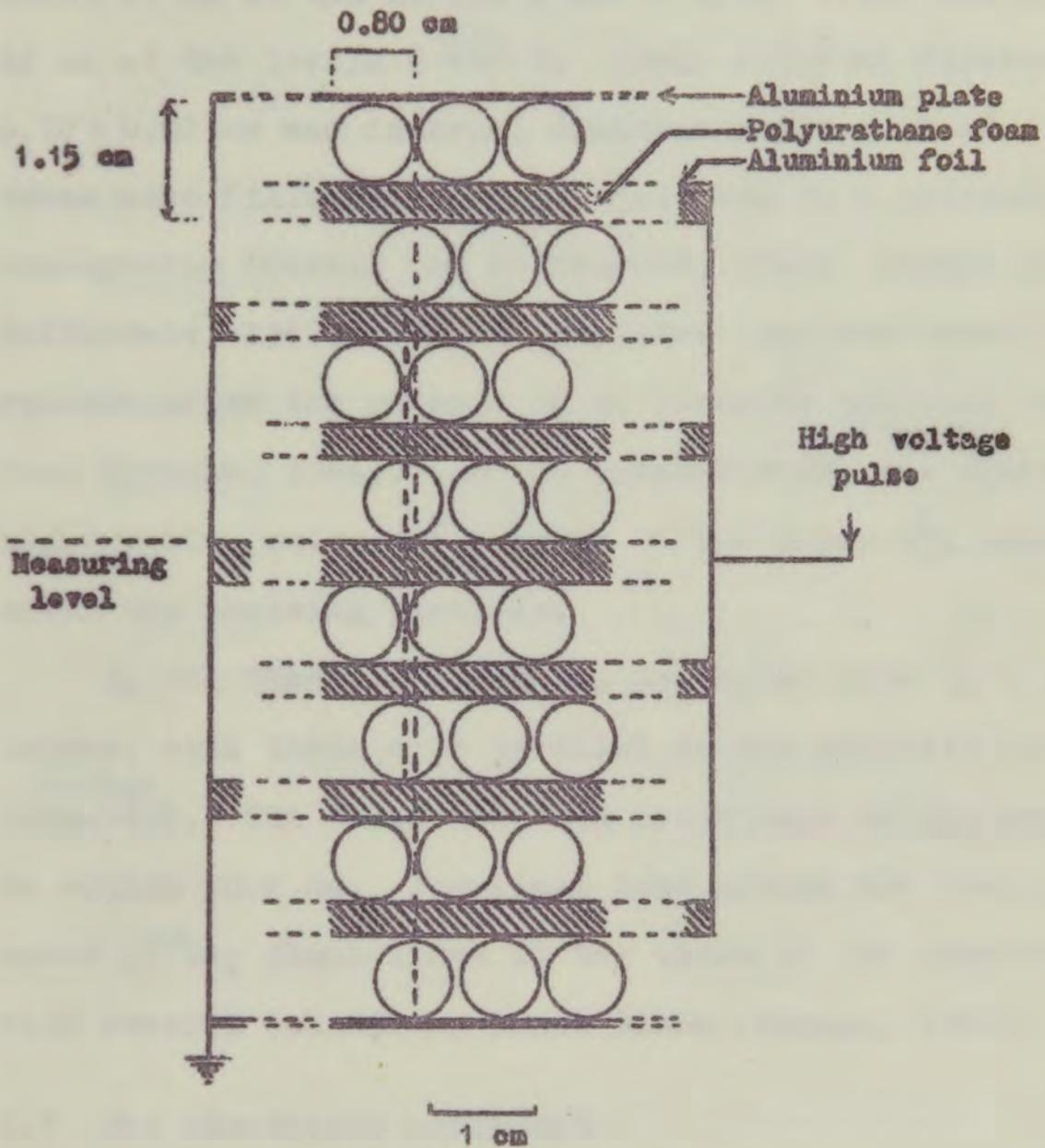
Fig. 2.2 A portion of a flash-tube array.

black except for a window at one end. Their lengths were about 67 cm at the levels A and D (Fig. 2.1), and about 42 cm at the levels B and C. Their external diameter was 0.72 ± 0.02 cm and internal diameter 0.59 ± 0.02 cm. The tubes were filled with commercial neon to a pressure of 2.3 atmospheres (Coxell and Wolfendale, 1960; Hayman and Wolfendale, 1962). Their sensitive time was about 39 microseconds after the passage of an ionizing particle through them (Brooke, 1964). In the present work, the operating high-tension pulse was applied to the tubes 15±1 microseconds after the ionizing particle.

In the flash tube arrays, the tubes were in 8 horizontal layers, with their axes parallel to the magnetic field (Fig. 2.2). The tubes had been positioned to the proper places to within ±0.2 mm. The flash tube arrays had been aligned by means of two plumb lines at the sides of the spectrograph, with several subsidiary plumb lines (Hayman, 1962).

2.3 The electronic equipment

A block diagram of the electronic equipment is given in Fig. 2.3. Most of the circuit diagrams and other details have been described by previous workers, Jones (1961), Jones et al. (1962), Hayman and Wolfendale (1962), Brooke (1964), and Palmer (1964). The circuit diagrams of those units which were
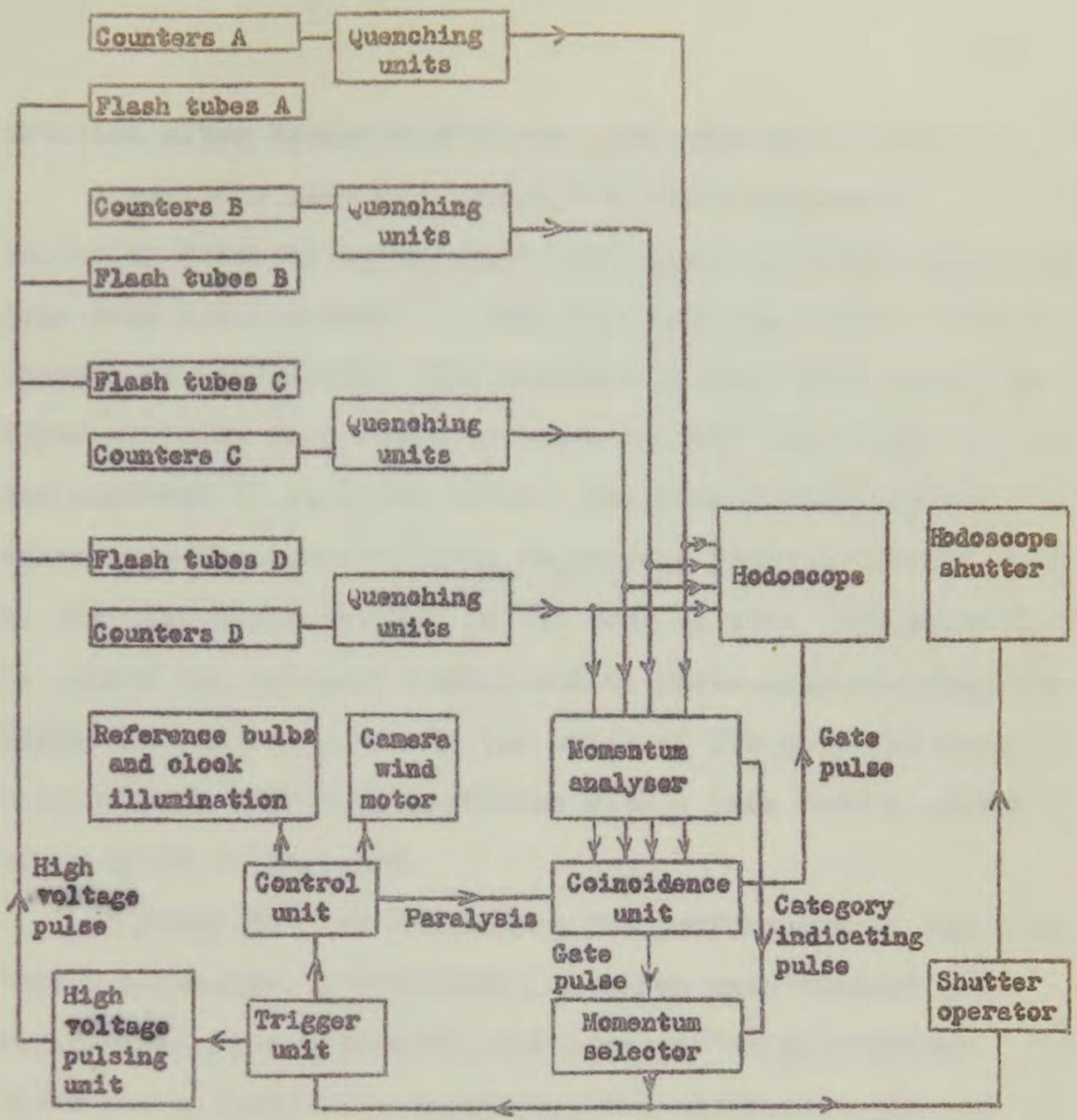
Fig. 2.3 Block diagram of the electronic equipment.

modified after Palmer's work are presented in Appendix 1.

A particle passing through the spectrograph was
initially detected by means of the Geiger counters, demanding
four fold coincidences, so that at least one counter was dis-
charged at each level. The counters of each tray were num-
bered serially from south to north so that the middle counter
was numbered 13 at every level. The 'momentum analyser'
determined the quantity $n = n_A - n_B - n_C + n_D$, where n_A is the number
of the discharged counter in the tray A, etc. The quantity n
is called the category number and it gives approximately the
deflection of the particle (in units of 3.8 cm). By means of
the momentum selector, particles with n less than a chosen
limit could be selected.

In order to have a check on the performance of the elec-
tronic selection, a hodoscope, in which each counter was
represented by a neon bulb, was constructed by Gijsbers. When
there was a fourfold coincidence, the bulbs corresponding to
the discharged counters were lit and gave a general picture of
the event.

2.4 The photographic recording

The flashes of the flash tubes were recorded by two
cameras (Fig. 2.1) in the usual way, i.e. the spectrograph
was in a darkened enclosure and the cameras could then be

used without shutters. The hodoscope had a separate shutter which was opened for the zero category events but remained shut during the other fourfold coincidences. After an accepted event, reference bulbs were illuminated at the edges of the flash tube arrays and hodoscope to assist in the iden--tification of the records on the film. Two clocks were also photographed to enable the corresponding AB and CD photographs to be found.

The sequence of operations when a particle passed through the spectrograph and satisfied the conditions required in the coincidence unit and momentum selector was as follows:

a) The coincidence unit was paralysed (see Fig. A1.2).

b) The high voltage pulse was applied to the flash tubes.

c) The relevant neon bulbs in the hodoscrope were lit and the shutter in front of it was opened.

d) The reference bulbs and the clocks were illuminated.

e) The cameras were wound on.

f) The paralysis was removed from the coincidence unit.

2.5 Equipment for scanning the photographic records

2.5.1 The projection system

For the analysis of the two data films a system of two projectors had been constructed. The films were projected onto movable boards on a table. On the boards, there were full-size charts of the flash tube arrays and hodoscope. In the chart of each array there was a scale immediately below the fourth tube-layer (Fig. 2.2). The tube spacing was used as the unit of the scale (1 t.s. = 0.8 cm).

To determine the location of the particle trajectory, the best estimate of the track was chosen by eye using a cursor. This determination is subsequently called the 'projection measurement'. The detailed rules of the projection measurement accepted for the present experiment are represented in section 3.4.1. According to previous work, the root-mean-square error in the track location in the projection measurement was at each level 0.091 ± 0.003 cm (Hayman, 1962).

2.5.2 The track simulator

In order to improve the accuracy of the track location for the high-energy muons, a "track simulator" had been constructed (Hayman and Wolfendale, 1962). This device

consisted of a model of a section of a flash tube array in which there was an enlargement by a factor of 10 in the horizontal direction and a factor 3 in the vertical direction. Each tube was represented by a slot behind which light bulbs were mounted. Over the face containing the slots there was a cursor.

An approximate way of taking into account the inefficiency of the flash tubes was provided as follows (Hayman, 1962): Marks had been drawn onto the slots to mark off 10% of the length of the slots at each end. The central part was assumed to have an efficiency of 100% . This means that the variation of the efficiency across a flash tube was approximated by a square function corresponding to the tube efficiency 80% found experimentally. The effect of this approximation on the accuracy of the track location was found to be small. The marks on the slots will subsequently be called "the efficiency marks".

The measuring procedure was as follows. The films were projected and the flashed tubes were noted. The pattern of tubes flashed in a tray around a chosen reference tube was reproduced on the simulator by switching on the appropriate bulbs. The direction of the trajectory was known to quite high accuracy from the projection measurements. Thus,

the cursor could be set at the correct angle by means of

a suitable scale. Then, usually a range of possible posi-

tions of the track was found, called the "corridor". Some

criteria had to be adopted for determining the best estimate

of the position. The criteria used in this work are given

in section 3.4.3. According to previous work (Hayman, 1962),

the root-mean-square error in the track location with the

track simulator was at each level 0.055 ± 0.002 cm.

2.6 Determination of the particle momenta

In Fig. 2.4, a schematic diagram is shown of the spectro-

graph and a particle trajectory. It is seen that a useful

measure of the deflection ϕ is the displacement

$$\Delta = \phi \, l_{,} .$$ 2.1

For small angles θ and ϕ, Δ may be approximately expressed

as follows:

$$\Delta = a - b - c + d - \Delta_o$$ 2.2

where $\Delta_o = a_o - b_o - c_o + d_o .$

This formula is derived in Appendix 2 where the effects

of the approximations are also evaluated. The values of the

geometrical constants are presented in connection with the

remeasurement of the dimensions of the spectrograph in
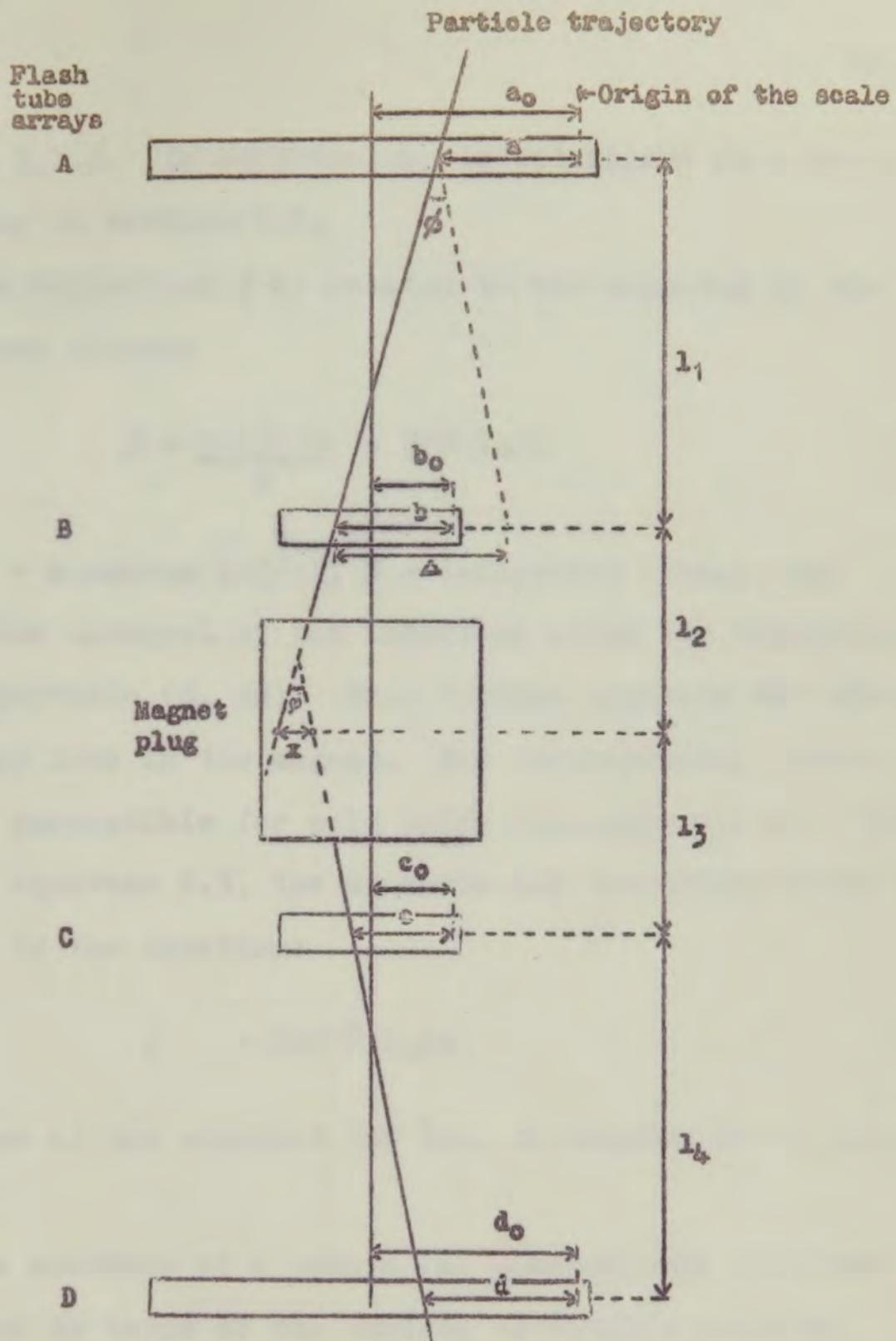
Fig. 2.4 Schematic diagram of the spectrograph and a particle trajectory.

section 3.1.2. In addition, Δ_o is determined in a statistical way in section 3.5.

The deflection $\emptyset$ is related to the momentum by the well-known formula

$$\emptyset = \frac{300\int Bdz}{p} = 300\ \bar{B}z/p \qquad 2.3$$

where p = momentum (eV/c), $\emptyset$ = deflection (rad.), and $\int Bdz$ = the integral of the induction along the trajectory of the particle (G. cm). This formula neglects the effect of energy loss in the magnet. The corresponding error becomes perceptible for p<20 GeV/c (see Appendix 5). According to equation 2.3, the momentum and the displacement are related by the equation:

$$p = 300\ \bar{B}zl_1/\Delta. \qquad 2.4$$

The value of the constant $300\ \bar{B}zl_1$ is determined in section 3.3.1.

The accuracy of a cosmic ray spectrograph is often expressed in terms of the maximum detectable momentum, defined as that momentum for which the magnetic deflection equals the probable error of the deflection. Instead of the probable error, the standard deviation is also sometimes used. According to an approximate determination (Palmer, 1964), the maximum detectable momentum of the Vertical

Durham Cosmic Ray Spectrograph was, after the installation

of the iron plug in the magnet, about 400 GeV/c, referring

to the probable error of the track-simulator technique.

CHAPTER 3

THE EXPERIMENT

3.1 Alignment of the spectrograph

3.1.1 The preliminary checks

Before starting the actual measurements, the alignment of the spectrograph was checked by means of the method of zero field runs used by previous workers (e.g. Hayman and Wolfendale, 1962). The total number of useful events in these runs was 1043. The resulting value for the mean Δ was -0.19 ± 0.10 cm. Because this value was not convincingly consistent with zero the geometrical dimensions of the spectrograph were remeasured.

A plumb-line system (Fig. 3.1) was constructed so that the position of the plumb lines could be directly observed at the measuring level of the flash tube arrays (Fig. 2.2). There were two such systems as seen in Fig. 3.1, one at the south side and one at the north side. The horizontal positioning of the flash tube arrays and of the counter trays were checked. Several small errors were found but they were in general inconsistent with the result of the zero field runs. To be sure, the horizontal positions of the detector

A — Reading telescope

←—Perlon line
(0.2 mm in diameter)

B ←— Loop of perlon line
held by drops of paint

West — Magnet plug — East

C

Brass rod
D ←— (4.8 mm in diameter)
←— Weight in damping oil
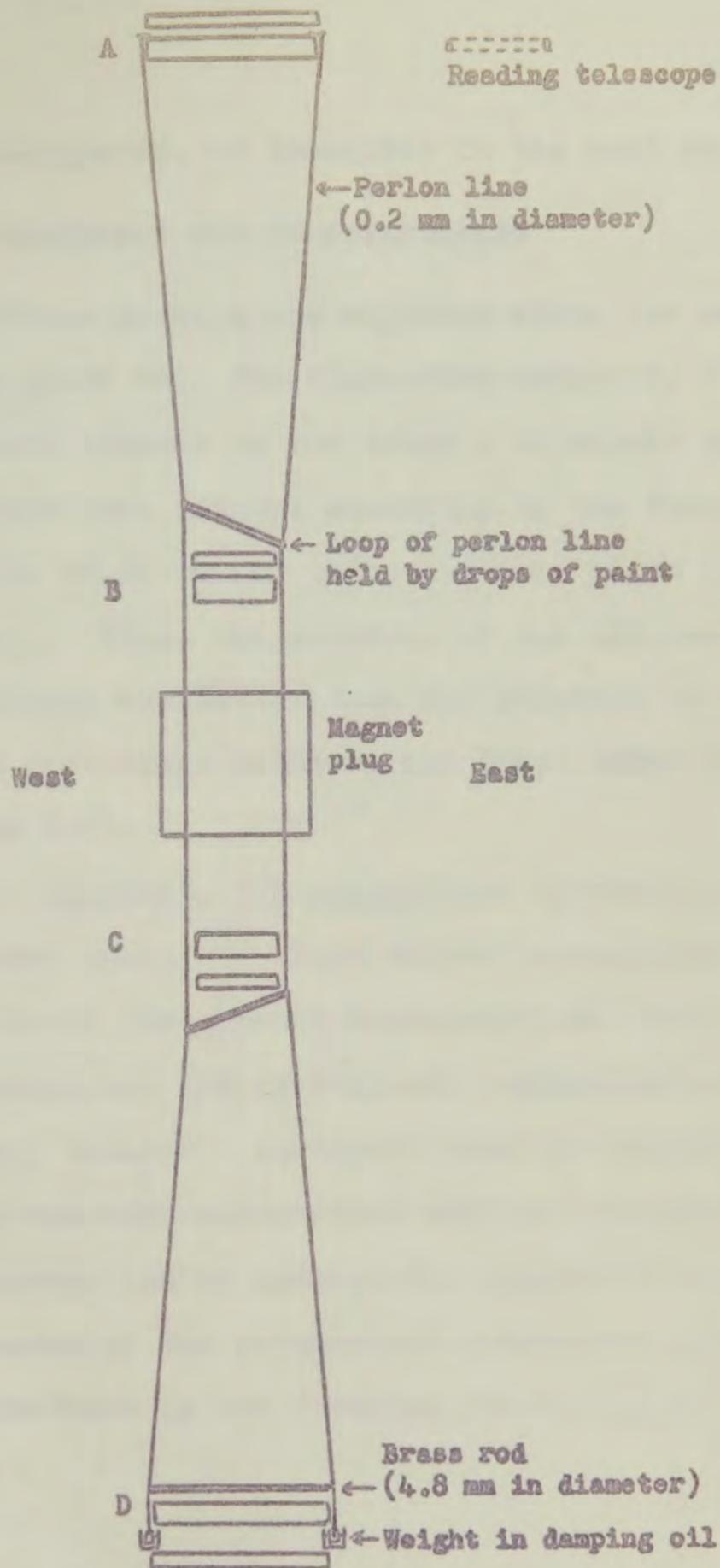
Fig. 3.1 The plumb-line system used for the alignment
of the spectrograph.

arrays were **re-adjusted**, as described in the next section.

3.1.2 The re-alignment and remeasurements

The flash-tube array A was adjusted above the magnet
plug to within ± 0.02 cm. The flash-tube arrays B, C and D
were aligned with respect to the array A to within ± 0.01 cm.
The counter trays were aligned according to the flash-tube
arrays to within ± 0.02 cm (by using auxliary plumb lines
where necessary). Thus, the accuracy of the alignment of
the detector arrays was better than the accuracy in the
positioning of individual counters and flash tubes in the
arrays (section 2.2).

After the alignment, the geometrical dimensions of the
spectrograph were measured. Four months later, after about
half of the runs of the present experiment had been carried
out, the alignment and the geometrical measurements were
again thoroughly checked. Agreement with the previous results
was found. It was also ascertained that the magnetic forces
in the spectrograph had no perceptible effect on the alignment.
The best estimates of the geometrical dimensions and of the
geometrical constants in the formulae of section 2.6 are shown
in table 3.1 .

Table 3.1

The geometrical constants (definitions

in section 2.6 and Appendix 2)

$l_1 = 189.56 \pm 0.016$ cm $\qquad L_1 = 193.62 \pm 0.03$ cm

$l_2 = 61.314 \pm 0.021$ cm $\qquad L_2 = 71.47 \pm 0.03$ cm

$l_3 = 60.002 \pm 0.030$ cm $\qquad L_3 = 72.14 \pm 0.03$ cm

$l_4 = 189.240 \pm 0.041$ cm $\qquad L_4 = 192.39 \pm 0.03$ cm

$$\Delta_o = 61.989 \pm 0.033 \text{ t.s.}$$

$$x_o = 0.498 \pm 0.023 \text{ t.s.}$$

$$z = 45.0 \text{ cm}$$

3.2 Measurement of the magnetic field

During the preparation stage of the present experiment

the average magnetic induction $\bar{B}$ in the effective part of

the magnet plug (Fig. 3.2) was measured by means of a flux-

meter and search coil by following the standard practice of

reversing the field. According to the measurements by

Gijsbers, $\bar{B} = 18.0$ kG for a magnetizing current of 59 A.

The pulses induced in the search coils were long (of the

order of 1 min.) and of peculiar shape, so that the correc-

tions for the restoring effect in the fluxmeter were large

(10 - 20%) and uncertain. After about 70% of the actual

runs of the spectrograph had been carried out, it was decided

to check $\bar{B}$. A new measuring method was accepted, as described

below.

The voltage V induced in the search coil D (Fig. 3.2) during the reversal of the field was measured as a function of time (t) by means of an oscilloscope. Then the average magnetic induction is:

$$\bar{B} = \tfrac{1}{2}(\int_0^\infty V dt)/NA \qquad\qquad 3.1$$

where N is the number of turns in the search coil (=25), and A is the area of the cross-section of the plug.

It was found that the stray field of the magnet affected somewhat the electron beam of the oscilloscope. A correction had to be determined by measuring the deviation of the beam when the input was disconnected but the magnet was switched on and off. It was also found that after switching off the magnetizing current the thermal demagnetisation of the iron had a significant effect. This effect was seen as a tail in the oscilloscope pulse, lasting about 150 sec. after the switching off. The tail caused by the self-induction lasted only for about 60 sec.

The result from some 20 experiments with a mean current of 60.2 A was $\bar{B}$ = 18.4 kG. The discrepancy between the result of Gijsbers' measurement and the present one is well within the estimate of random errors. To obtain the best estimate
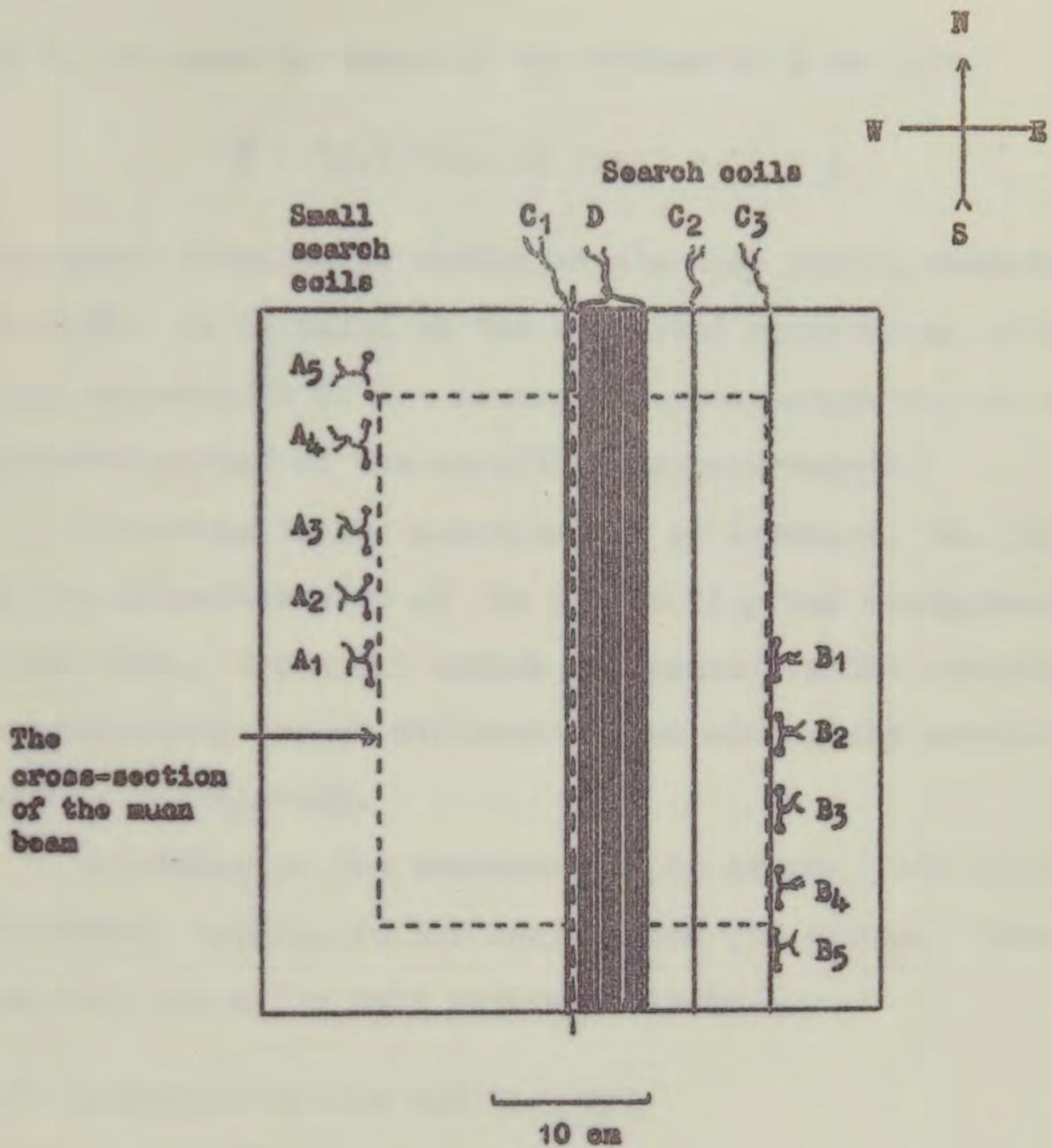
Fig. 3.2 The iron plug of the electromagnet
seen from above.

of $\bar{B}$, the mean is taken of the values of $\bar{B}$ to give

$$\bar{B} = 18.2 \pm 0.5 \text{ kG for I} = 59.6 \text{ A}$$

The error shown is an estimated standard error, amounting to 2.7%. It is based on the estimated uncertainty of the time corrections of the fluxmeter measurements and on the observed spread of the oscilloscope measurements.

According to the measurements by Gijsbers, the field in the effective part of the magnet plug was homogeneous within $\pm 3\%$. The small errors in Δ caused by the existing inhomogeneity are of different signs and should cancel out in statistical work.

According to the measurements by Kamiya, $\Delta\bar{B}/\Delta I$ was 0.043kG/A, 0.2%/A, in the region from 51A to 61A. Thus, the iron was quite well saturated at 60 A.

3.3   Operation of the spectrograph

3.3.1   General procedure

In order to obtain large deflections of the particles and a steady, saturated field, the magnetizing current was set up to its nominal maximum value 60 A. For the purpose of avoiding instrumental biases, the standard practice of reversing the magnetizing current between separate runs was followed. The field direction from east to west was called

positive. As the interest was in the high-momentum muons only, the momentum selector was set to accept the events of the category zero and to reject the others. The actual setting of the bias in the discriminator valves corresponded to ± 0.6 category units.

The collection of the basic data was carried out during the period between June, 1964 and January, 1965. The total running time was about 3000 hours. The useful times for positive and negative fields were 1382 and 1421 hours, respectively, in a satisfactory balance. The operation involved 109 separate runs, each of which lasted for one or two days depending on practical circumstances. Some 720000 four-fold coincidences were recorded of which about 34000 were selected and photographed as category zero events. The rate of four-fold coincidences was, on the average, 3.96/min. and it did not vary much. The mean rate of the category-zero events was 0.19/min. This value was found to vary somewhat with time. A chi-squared test for a sample of 15 consecutive runs yielded the result $x^2 = 39.9$ and thus the possibility of the variations being due simply to Poisson fluctuation was only of the order of 0.1%. More probably there was extra variation caused by some instability in the electronics. However, this variation could not affect the frequency distribution of the particle deflections within category zero.

The mean of the magnetizing current was 57.8 A, as evaluated from the readings of the current at the beginning and end of the runs. This mean value is so close to the mean current used in the field measurements (59.6 A), that variation of $\bar{B}$ need not be taken into account. Using the geometrical constants given in table 3.1, the constant $300\ \bar{B}z l_i$ becomes 58.2 (GeV/c) (t.s.). Because of the fluctuation in the mains, the ageing of the rectifiers, and other changes in conditions, the current varied within ± 3.0 A from the mean. The corresponding limits for $\bar{B}$ were ± 0.13 kG. The corresponding fluctuation in the particle deflection is negligible.

During the dismantling of the electromagnet after the experiment it was found that for some reason considerable heat damage had happened to the supports of the current coils. Some leak currents had probably occurred. However, as no significant increase was found in the total current during the experiment and no decrease in magnetic field compared with previous measurements, the leakage has not been serious.

3.3.2 Daily checks

Before every run the values of the supply voltages, discriminator voltages, and the magnetizing current were checked, and the functioning of the counters, flash tubes,

hodoscope, and the recording system (cf. section 2.4) was tested. During each day, the values of certain supply voltages, the magnet current and the rates of the four-fold coincidences and category-zero events were checked at intervals of a few hours. After the runs the films were examined visually and, in particular, the efficiency of the flash-tubes was checked. For a few runs at the beginning of the experiment, the efficiency was checked by calculating the mean number of flashes in an array. For the arrays A, B, and C the mean number was close to 5, for D it was about 4.4. Later, the stability of the efficiency was checked by counting the number of those events when only 2 flashes occurred in D. This number varied randomly between 1% and 9% of the total number of events in a run but no systematic deterioration of the efficiency was found.

3.4. The scanning of the photographic records

3.4.1 The projection measurements

To be accepted for the projection measurements, an event had to satisfy each of the following requirements: First, one and only one flash was to be unambiguously seen at every tray in the hodoscope. Second, the category number calculated according to the hodoscope flashes was to be zero.

Third, one track was to be unambiguously seen in each
flash tube array. However, if a knock-on electron had
been produced within an array and the electron could be
distinguished from the muon, the event was also accepted.
Finally, the number of flashes was to be≥ 3 in each array.

For an accepted event, a, b, c, and d were measured
to the nearest 0.1 t.s. At this stage the selection of the
most probable location of the track was not done according
to any strict criteria. However, as far as it was possible
by eye, the angle of the cursor was set to be equal in arrays
A and B and again in arrays C and D. Allowance was made for
the few flash tubes which were known to be not working. A
standard check was that the flash in the D tray of the hodo-
scope had to agree with the location of the track in the
flash tube array D.

Finally, Δ was calculated according to the equation
2.2, using for Δ_e the value 62.0 t.s. obtained from the
geometrical measurements (table 3.1). According to the same
measurements the upper limit of Δ was 8.15 t.s. However,
because of some technical failures in a few cases, amounting
to some 0.5% of the total, Δ was > 8.15 t.s. These events
were rejected.

3.4.2 The displacement distribution from
the projection measurements

In order to obtain the statistical frequency distributions of particle deflections mentioned in section 2.1, the particles were histogrammed in fixed cells of displacement Δ. It was found necessary to use individual values of Δ as cells, i.e. the cell width was 0.1 t.s., defined by the accuracy of the scale reading (section 3.4.1). This method made it convenient to join the cells later to form different cell systems according to the need (section 4.2). By taking into account the direction of the magnetic field, the events were histogrammed so that positive muons were on the side of positive Δ and vice versa. The resulting histogram is shown by table 3.2 and by figure 3.3.

3.4.3. The track-simulator measurements

The procedure of the track-simulator measurements was established by Hayman and Wolfendale (1962) and has already been described in section 2.5.2. In the present work only certain details of the working rules were changed. In particular, the criteria needed for determining the corridor were reconsidered, taking into account the following requirements:
1) The middle of the corridor should coincide with the mean of the probability distribution of the location of the trajectory. 2) Half of the width of the corridor should give the first approximation of the standard deviation of that distribution. 3) The criteria should define the corridor objectively.

4) To make the measurement quicker the criteria should be simple, even at some cost in accuracy.

Table 3.2 The observed displacement distributions

Cells (t.s.)	From projection measurement		From track-simulator measurement	
	μ_+	μ_-	μ_+	μ_-
0 - 0.05		67		51
0.05 - 0.15	58	76	54	48
0.15 - 0.25	92	78	69	57
0.25 - 0.35	100	78	92	84
0.35 - 0.45	139	94	118	77
0.45 - 0.55	146	102	133	107
0.55 - 0.65	170	136	158	134
0.65 - 0.75	184	156	177	146
0.75 - 0.85	184	185	155	146
0.85 - 0.95	245	187	217	163
0.95 - 1.05	257	196	179	149
1.05 - 1.15	274	199	174	112
1.15 - 1.25	257	214	116	108
1.25 - 1.35	267	205	75	66
1.35 - 1.45	300	217	42	31
1.45 - 1.55	299	226	26	17
1.55 - 1.65	288	234	11	9
1.65 - 1.75	303	237	1	5
1.75 - 1.85	273	232	3	3
1.85 - 1.95	298	238		
1.95 - 2.45	1437	1187		
2.45 - 2.95	1314	1014		
2.95 - 3.45	1118	863		
3.45 - 3.95	874	721		
3.95 - 4.45	611	504		
4.45 - 4.95	490	360		
4.95 - 5.45	297	242		
5.45 - 5.95	177	138		
5.95 - 6.45	118	86		
6.45 - 6.95	58	47		
6.95 - 7.45	24	25		
7.45 - 7.95	12	16		
7.95 - 8.15	5	6		
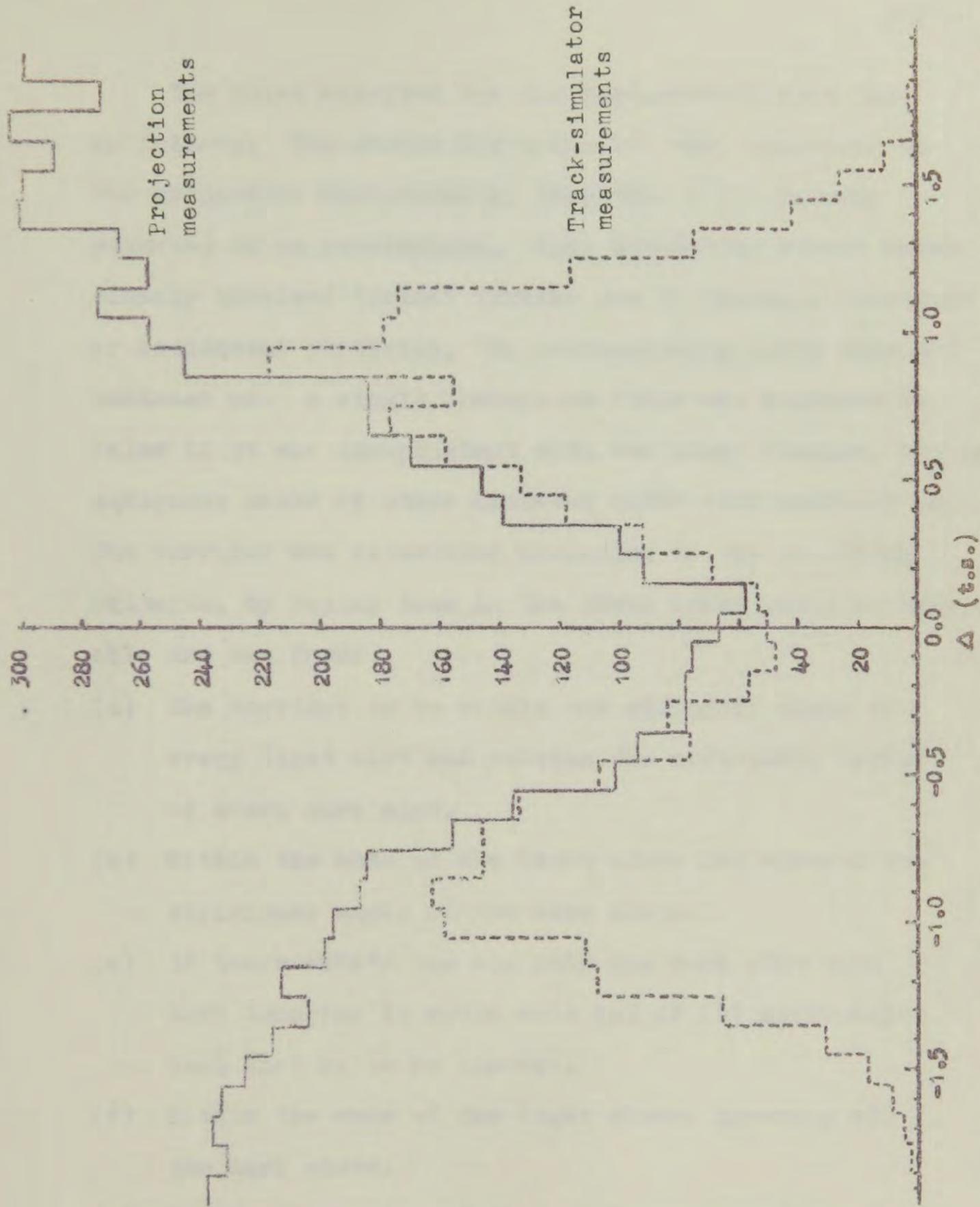
Fig. 3.3 Comparison between the displacement distributions from the projection measurements and the track-simulator measurements.

The rules accepted for the measurements were then as follows: The events for which $|\Delta|$ was, according to the projection measurements, less than 1.2 t.s. were selected to be re-examined. When simulating events which clearly involved "false" flashes due to knock-on electrons or accidental particles, the corresponding bulbs were not switched on. A single suspicious flash was regarded as false if it was inconsistent with two other flashes, but in ambiguous cases of other kinds the bulbs were switched on. The corridor was determined according to the following criteria, by trying them in the given order until an applicable one was found:

(a) The corridor to be within the efficency marks of every light slot and outside the efficiency marks of every dark slot.

(b) Within the ends of the light slots and outside the efficiency marks of the dark slots.

(c) If there exists one and only one dark slot such that ignoring it would make (a) or (b) applicable, that slot is to be ignored.

(d) Within the ends of the light slots, ignoring all the dark slots.

(e) For the left edge of the corridor, the rightmost inconsistent slots are to be ignored and then
   (d) is to be used. For the right edge, the leftmost

inconsistent slots are to be ignored and (d)

is to be used.

In every case, the location of the edges of the corridor
were noted down in tube spacings with two decimal places.
If the width of the corridor was greater than 0,3 t.s.
at any flash tube array, the event was rejected. For the
other events, the location of the corridor was calculated.
The values thus obtained are denoted by a_{tr}, b_{tr}, c_{tr}, and d_{tr}.
According to them, the quantity $\Delta_{tr} = a_{tr} - b_{tr} - c_{tr} + d_{tr} - \Delta_o$
was calculated.

3.4.4 The displacement distribution from the
track-simulator measurements

The track-simulator data were histogrammed by using
the same cell division as in the histograms of the projection
measurement. The events which lay on a cell limit were
treated as follows: If the inclination angle of the trajec-
tory in the spectrograph was positive, the event was marked
into the cell of lower Δ and vice versa. This rule was
suggested by the small "inclination error" found in Appendix 2.

The resulting histogram is shown by table 3.2. For the
sake of comparison it is also drawn in figure 3.3. The compari-
son proves that in the range from -0,7 to 0.7 t.s., the shape
of the two histograms is nearly the same taking into account

the Poisson fluctuation. This means that in the present
experiment the large scattering has made the track simula-
tion inefficient.

3.5   Statistical check on the geometrical constant Δ_o

If the Δ-histogram is drawn without changing the sign
of Δ according to the reversals of the magnetic field, the
minimum of the histogram should lie at $\Delta = 0$. An error in
Δ_o would result in a deviation from zero. This fact was
used to check the value obtained from the geometrical measure-
ments, Δ_{oG} .

The track-simulator data were used for this check,
because they should, in theory, exhibit sharper minimum
than the projection data. (According to Fig. 3.3 this
choice was not so important.) Only the range from -0.9 to
0.9 t.s. was used, since the range $|\Delta| > 0.9$ t.s. depended
on the geometrical Δ_o through the selection of the high-
momentum events. At the time of this check, the scanning
of the films was still going on, but 84% of the data were
ready and could be used.

Several methods were tried for the determination of
Δ_{os} (the statistical Δ_o). Firstly, the observed displacement
histogram was smoothed by the fourth differences
(e.g. Scarborough, 1950, p. 459). It was found that this

method did not give sufficient weight to the requirement
of symmetry in the displacement distribution. In addition,
the estimation of the standard deviation of the location of
the minimum was rather arbitrary. Secondly, curve fitting
was tried. Polynomials were used as fitting functions,
dropping the terms which were asymmetric with respect to
the minimum. The statistical errors of the observed histo-
gram were so large that it was difficult to decide how many
terms of the polynomial would be significant. It was felt
that the shape of the curve should be defined by more realistic
means. So these trials lead to the following prodedure.

The shape of the expected displacement distribution was
determined by the scattering calcuations, which are considered
in detail in section 4.2.4. The rounding of the cut-off edge
at the selection limit 1.2 t.s. was taken into account accord-
ing to a statistical study on the deviation of the track-
simulator Δ from the projection Δ. The theoretical distribu-
tion was fitted to the observed data by using Δ_0 and E as the
adjustable parameters, E being the overall efficiency of the
experiment. The value obtained for Δ_{os} was 61.968 ± 0.045 t.s.
The value of x^2 was 20.6, corresponding to 20% level of signi-
ficance. The level is high enough to justify the accepted
method.

Next, Δ_{os} is compared with Δ_{oG}, which is given in table 3.1. To be more precise, a correction of 0.02 t.s. is added to Δ_{oG} to allow for the small tilt error found in Appendix 2. Then, Δ_{oG} is 62.009 t.s. with a standard deviation of about 0.035 t.s. The agreement between Δ_{os} and Δ_{oG} is good.

Both Δ_{os} and Δ_{oG} give significant independent information of the constant Δ_o. The best value would be their weighted mean, which is 61.994 t.s. Hence the best practical value is still $\Delta_o = 62.0$ t.s., as used in section 3.4.

3.6 The uncorrected results on the charge excess

By virtue of the symmetry of the spectrograph, both positive and negative muons should be accepted evenly. Neglecting the Coulomb scattering and other noise in Δ, i_+ and i_- in equation 1.1 could be replaced by the corresponding counting rates N_+ and N_-. Then, the first approximation of R is obtained:

$$R_I = N_+ / N_- . \qquad 3.2$$

Assuming that the statistical errors in the counting rates are Poissonian, the standard deviation of R_I is:

$$\sigma = R_I (N_+^{-1} + N_-^{-1})^{\frac{1}{2}} . \qquad 3.2$$

The values of R_I obtained from the projection data are shown in table 3.3. For the high momentum cell, where the location errors could be expected to matter, R_I is also given according to the track-simulator data. It is seen that the track-simulator technique did not make any significant difference.

Table 3.3   The first approximation of the charge ratio, R_I

Cell limits (t.s.):	0.15	0.45	0.75	1.05	1.95	3.45	8.15
R_I		1.32	1.27	1.21	1.28	1.26	1.24
σ		0.11	0.085	0.069	0.038	0.031	0.036
R_I (track simulator)	1.28						
σ (track simulator)	0.12						

CHAPTER 4

METHODOLOGICAL CORRECTIONS

4.1 The acceptance functions of the spectrograph

4.1.1 Introduction

As mentioned already in section 2.1, the observed
displacement distribution was to be corrected for the
variation of the acceptance with Δ. According to Brooke
et al. (1962) and Hayman et al. (1963), the observed dis-
tribution $S_0(\Delta)$ is related to the scattered displacement
distribution $N(\Delta)$ by the equation:

$$S_0(\Delta) = N(\Delta).E.A(\Delta).G(\Delta).B(\Delta) \qquad\qquad 4.1$$

where E is the efficiency of the detector system, $A(\Delta)$ is
the so-called acceptance function, $G(\Delta)$ is the so-called
elementary function, and $B(\Delta)$ is the bias function. Accord-
ing to the experiences of previous workers, E can be assumed
to be independent of Δ (Gardener et al., 1962; Hayman and
Wolfendale, 1962). Since this experiment was only designed
to determine a normalized momentum spectrum and relative
charge excess, the results do not depend on E. The functions
$A(\Delta)$, $G(\Delta)$, and $B(\Delta)$ have an effect on the spectrum, and they
will now be evaluated.

4.1.2 The acceptance function $A(\Delta)$

The function $A(\Delta)$ is the integral over the solid angle ω and the area q within which the spectrograph collected particles:

$$A(\Delta) = \iint dq \, d\omega. \qquad 4.2$$

The integral can be taken at any convenient level in the spectrograph . Because of the symmetry of the spectrograph $A(-\Delta)$ equals $A(\Delta)$ and so this function has no effect on the measured charge ratio. The calculation of $A(\Delta)$ for the present experiment is performed in Appendix 3, and the results are given in table 4.1. It is seen that $A(\Delta)$ is nearly constant for the muons of category zero accepted in the experiment (section 3.3.1).

Table 4.1 Values of the acceptance functions

Δ (t.s.)	$A(\Delta)$ (27 cm^2 sterad)	$G(\Delta)$	$B(\Delta)$
0	1.000	0.478	0.86
0.3	1.000	0.472	0.85
0.5	1.000	0.468	0.83
1	1.000	0.441	0.84
2	0.999	0.353	0.85
3	0.998	0.241	0.86
4	0.996	0.135	0.86
5	0.994	0.062	0.86
6	0.992	0.021	0.87
7	0.989	0.004	0.87
8	0.985	0.000	0.87

4.1.3 The elementary function $G(\Delta)$

The elementary function gives the probability that a particle passing through the spectrograph within the allowed area and solid angle was recorded in the category zero. According to previous workers (e.g. Brooke et al., 1962), this probability may be expressed as follows:

$$G(\Delta) = 2\{2(r_1 - s|\Delta|/2)^3 - (r_1 - s|\Delta|)^3\}/3r_2^3 \quad \text{for} \quad |\Delta| \leq r_1/s;$$
$$G(\Delta) = 4(r_1 - s|\Delta|/2)^3/3r_2^3 \quad \text{for} \quad r_1/s \leq |\Delta| \leq 2r_1/s, \qquad 4.3$$

where $s = (L_1 + L_4)/4l_1$ (see table 3.1). The quantities $2r_1$ and $2r_2$ are the internal diameter and lateral separation of the Geiger counters, respectively ($r_1 \approx 1.7$ cm, $r_2 = 1.9$ cm). It is seen that $G(\Delta)$ also has no effect on the measured charge ratio. Values of $G(\Delta)$ are given in table 4.1. It should be mentioned that because of the considerable uncertainty in r_1, the standard error of the absolute values of $G(\Delta)$ may be as high as 0.03. However, in the present experiment only the relative values $G(\Delta)/G(0)$ matter, and according to previous experience these values are accurate enough (Gardener et al., 1962; Hayman and Wolfendale, 1962).

4.1.4 The bias function B(Δ)

The function $B(\Delta)$ in equation 4.1 allows for the bias which arose from the rejection of events with two or more simultaneous particles at one or more detector levels. The

main types of such events were as follows (Palmer, 1964):

(i)   A muon generated a knock-on electron in the
        spectrograph.

(ii)   A muon was part of an extensive air shower, and
        the shower electrons were recorded together with
        the muon.

(iii)   Two muons were sufficiently close to each other
        to pass together through the effective area of
        the spectrograph.

        The majority of these accompanied muons were rejected
by the momentum selector because the pulse representing the
category number was usually far from zero if two or more
counters were discharged in one tray. Further accompanied
muons were rejected during the scanning of the films in
order to avoid ambiguous measurements (section 3.4.1). These
rejection procedures can be expected to reduce the number of
positive and negative muons in the same proportion. Conse-
quently they should not affect the charge ratio. In the
momentum spectrum the normalization reduces the bias and
some error is generated only if the bias varies with Δ.
Now, the relative frequency of the accompanied muons is known
to increase with momentum, mainly because of the incident
showers (Hayman et al., 1963; Palmer, 1964). Thus there will
be some bias at high momenta. In equation 4.1, the bias can

be conveniently considered as variation of the acceptance
of the apparatus with varying Δ.

Palmer studied the bias effect in the same spectrograph
as used in the present work. He collected some 4000 events
without using the momentum selector and measured the dis-
placement for the accompanied muons, as far as possible.
He worked out the ratio of accompanied to single muons in
terms of integral spectra. The function $B(\Delta)$ is calculated
from Palmer's results in Appendix 4 and the resulting values
are shown in table 4.1. It should be pointed out that Palmer
did not make any scattering correction and therefore the
corresponding bias function should apply expressly to the
scattered distribution $N(\Delta)$ used in equation 4.1.

4.2 The correction for the noise in Δ

4.2.1 Introduction

In previous works, two different methods have been used
in the correction for errors in the measured displacements Δ.
Firstly, the statistical standard deviation of Δ may be deter-
mined quite accurately and consequently the effect of these
errors on the results may be estimated theoretically
(e.g. Brooke, 1964). Secondly, the particles with erroneous Δ
may be found by suitable check measurements and they can be
then rejected. For instance Hayman and Wolfendale (1962)

used the "discrepancy" x defined in Appendix 2 to detect

events with large errors.

4.2.2 Detection of the noise by means of the discrepancy x

The discrepancy x was calculated for the events of

several runs in the beginning of the experiment. Setting

the upper limit of $|x|$ at 2.00 t.s. it was found that only

6 events had to be rejected out of 973. Furthermore, these

events should be attributed rather to accidental coincidences

than to large scattering. Therefore, a special test was per-

formed on the usefulness of this method in the high-momentum

range $0 \le |\Delta| \le 0.4$ t.s. Rejecting events with $|x| > 0.3$ t.s.

removed 20 events out of 82, which is 24%. However, it was

estimated by the aid of the theoretical methods, which will

be explained in the next two sections, that according to the

OWP-spectrum the reduction should be 41% at the limit

$|\Delta| = 0.4$ t.s. and it should obviously increase to 100% at $\Delta = 0$.

This proved, in spite of the poor statistics, that the errone-

ous events could not be efficiently revealed by means of x.

Also the possibility of rejecting part of the scattered muons

was abandoned because it would have made the theorectical esti-

mation of the remainder more complicated. Furthermore, the

revealing of the few accidental events was not considered

worth much effort as the scattering was clearly a much greater source of error. So the calculation of x was ceased altogether. The reason for the failure of this method is the fact that in the present experiment the noise occurred mainly at the centre of the spectrograph and not at the detector levels as in the work of Hayman and Wolfendale. It should be pointed out, however, that the method of detecting scattering or other noise by checking against inconsistency in the particle trajectory can be applied to spectrographs with solid iron magnets if certain special design is used (e.g. Rochester et al., 1965; MacKeown et al., 1965 a).

4.2.3 The root-mean-square error of Δ

The effect of Coulomb scattering in the magnet on the magnetic or true displacement Δ_t is estimated according to the theory of Ashton and Wolfendale (1963). The theory gives the mean square (projected) displacement $\langle y^2 \rangle$ taking into account the momentum loss in the magnet. The quantity $\langle y^2 \rangle$ is calculated for the present spectrograph in Appendix 5. The resulting values are given in table 4.2.

The mean square value of the location error of the projection measurement or the track simulator measurement can be added to $\langle y^2 \rangle$ because their effect on Δ_t is similar. These

values are $0.055(t.s.)^2$ (section 2.5.1) and $0.019(t.s.)^2$ (section 2.5.2), respectively. Because of the steep slope of the momentum spectrum which favours the Coulomb scattering from low momenta, these errors were rather un- important. The small geometrical errors found in Appendix 2 contribute only about $0.003(t.s.)^2$ and are thus negligible. The root-mean-square value of the total error, σ, is shown in table 4.2 for both the projection and track-simulator tehcniques. For $|\Delta|>3$ t.s., σ is in both cases about 31% of the magnetic displacement.

Table 4.2. The root-mean-square error of Δ_t for the projection measurement (σ_{pr}) and for the track-simulator

measurement (σ_{tr})

Δ (t.s.)	$\langle y^2 \rangle$ (t.s.)^2	σ_{pr} (t.s.)	σ_{tr} (t.s.)
0	0	0.240	0.146
0.116	0.0013	0.243	0.151
0.291	0.0081	0.256	0.172
0.582	0.0324	0.300	0.232
1.17	0.1325	0.436	0.392
2.99	0.855	0.956	0.936
6.13	3.61	1.92	1.92
13.1	16.0	4.00	4.00
39.1	142	11.9	11.9
120	1400	37.4	37.4

4.2.4 The scattering correction according to the

OWP spectrum

A common practice in the scattering correction has
been to adopt a comparison spectrum, calculate the scatter-
ed spectrum, compare the calculated and the observed spectra,
and then modify the comparison spectrum if necessary
(e.g. Hayman and Wolfendale, 1962). When dealing with the
momentum spectrum without distinguishing between the positive
and negative muons, the scattered Δ-distribution can be
expressed as:

$$N_{tot}(\Delta) = N(+\Delta) + N(-\Delta) = \int_0^\infty i(\Delta_t)\sigma^{-1}\varphi[(\Delta - \Delta_t)\sigma^{-1}]d\Delta_t \quad 4.4$$

where σ is the root-mean-square error of Δ_t (section 4.2.3)
and $\sigma^{-1}\varphi[(\Delta - \Delta_t)\sigma^{-1}]$ is the fraction of muons which scatter
from Δ_t to Δ. According to the theory of the multiple
scattering, φ is closely Gaussian (e.g. Rossi, 1961, p. 69).
The integration can be conveniently performed by dividing
the distribution $i(\Delta_t)$ into cells, keeping the cell width
considerably smaller than σ (Brooke, 1964). Then, the intensity
in each cell is replaced by a Gaussian distribution with the
appropriate area and σ. The contributions from these dis-
tributions are summed up at selected points Δ. The expected
accepted spectrum is then obtained according to equation 4.1.

In the present work, the OWP spectrum (Osborne et al.,
1964) was used as the comparison spectrum. In the first
place, calculation was made for the track-simulator work and

the corresponding location error was adopted. About 60
cells were used in the integral, and $N(\Delta)$ was summed up
at 11 points, ranging from -0.5 to 6 t.s. The resulting
distribution $S_o(\Delta)$ was used for the check on Δ_o explained
in section 3.5. As mentioned there, the calculation showed
as a side result that the expected and observed distributions
in the range p > 65 GeV/c agreed with 20% level of signifi-
cance. It should be recalled that this test referred only
to 84% of the total running time.

During the calculation of $N(\Delta)$, it was found that in
the range $\Delta > 0.5$ t.s. the effect of the location error was
negligible. It was estimated that the change to the location
error of the projection technique could not make much differ-
ence below 0.5 t.s. either. This conclusion was supported
by the comparison of the observed distributions (Fig. 3.3).
Therefore, the existing values of $N_{tot}(\Delta)$ were accepted for
the correction of the projection data as well. The scatter-
ing correction on the differential momentum spectrum can be
represented by means of the ratio of the unscattered spectrum
to the scattered one. This ratio is shown in table 4.3. By
integrating $N_{tot}(\Delta)$, scattering corrections can be obtained
for the integral momentum spectrum. In this case, it is
convenient to include the acceptance functions and normaliz-
ation to the same correction factors. These are also shown
in table 4.3.

Table 4.3 The scattering corrections æ for the differential

and integral spectra

Δ (t.s.)	$æ_1 = \dfrac{i_{owp}(\Delta)}{N(\Delta)}$	$æ_2 = \dfrac{I_{owp}(<\Delta)\ S_0(<8.15\ t.s.)}{I_{owp}(<8.15\ t.s.)\ S_0(<\Delta)}$
0.2	0.450	
0.5	0.626	0.165
1	0.736	0.214
2	0.820	0.303
3	0.860	
4	0.900	
5	0.94	
6	0.95	
8.15	–	1.000

The effect of the scattering was studied further by
determining the distribution of the true or magnetic dis-
placement Δ_t of the muons which had an observed displacement
Δ. This distribution is denoted by $f(\Delta, \Delta_t)$. Fig. 4.1 shows
the median and quartiles of $f(\Delta, \Delta_t)$ as function of Δ in the
high-momentum region. The figure emphasizes the seriousness
of the scattering effect. A point of interest is the mini-
mum of Δ_t which determines a kind of upper limit for the
momenta reached by the spectrograph.

4.2.5. The scattering correction according to the

previous best estimate of the charge excess

The best estimate of the charge ratio in the vertical
direction was based on the survey performed by MacKeown
et al. (1963). Taking into account the speculations of the
different production mechanisms of muons, the unsure minimum
and high-momenta rise were incorporated into the estimate
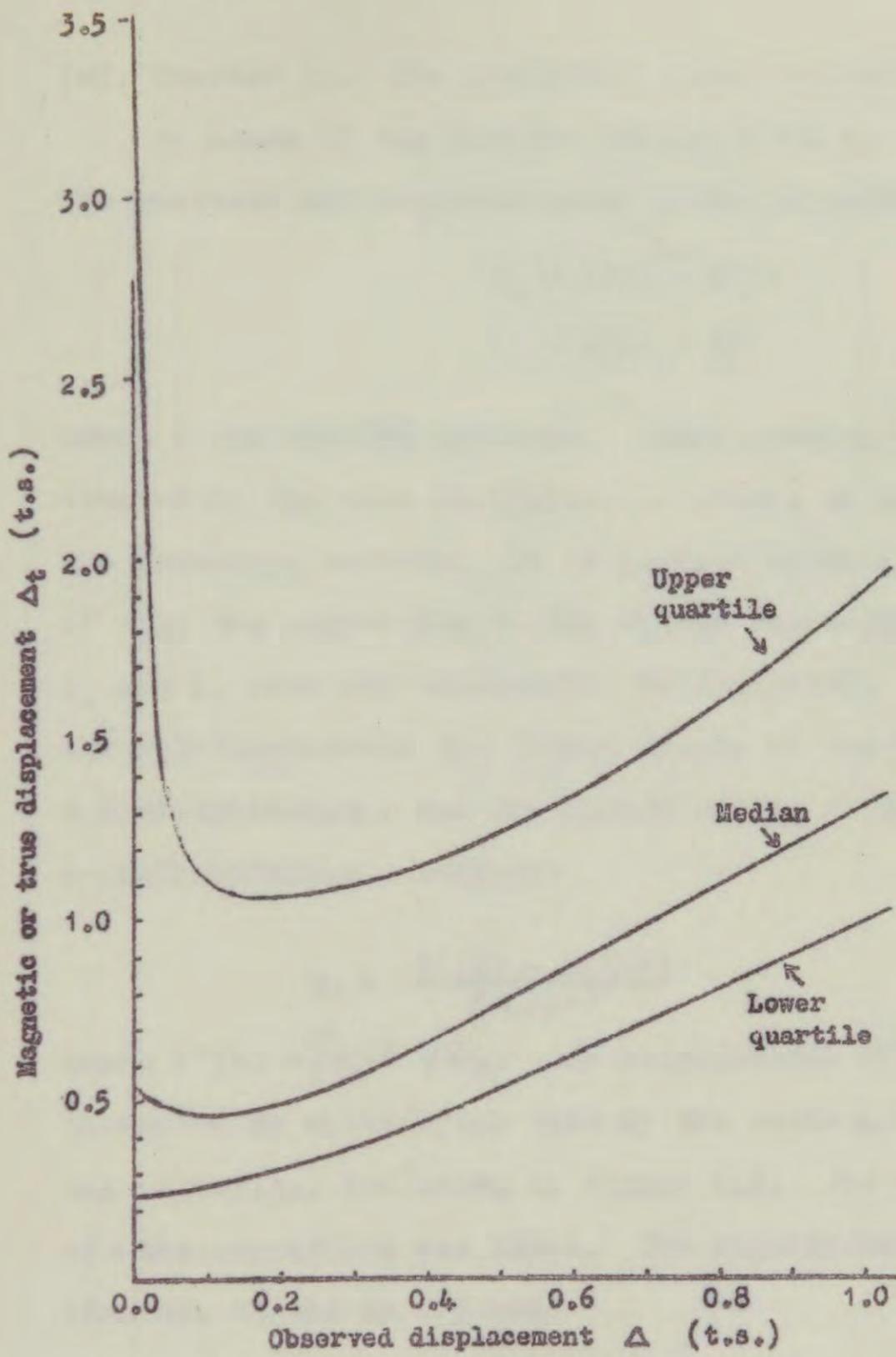
Fig. 4.1   The median and quartiles of the function $f(\Delta, \Delta_t)$ as a function of Δ.

(cf. Chapter 1). The resulting curve is shown in Fig. 4.2.

By means of the adopted charge ratio R, the spectra of the positive and negative muons could be separated as follows:

$$i_+ = i/(1 + R^{-1})$$
$$i_- = i/(1 + R)$$

4.5

where i was the OWP spectrum. These spectra could then be treated by the same scattering procedure as explained in the preceding section. It is perhaps worth mentioning that if only the correction to the charge excess is required, i_+ and i_- need not necessarily be separated. In this case the relation between the charge excess of the unscattered Δ-distribution, η_u, and the charge excess of the scattered Δ-distribution, η_s, becomes:

$$\eta_s = \cdot \frac{N'(\Delta) - N'(-\Delta)}{N_{tot}(\Delta)}$$

4.6

where $N'(\Delta) = \int_0^\infty \eta_u i \sigma^{-1} \varphi \, d\Delta_t$. The experimental values η_x were corrected by multiplying them by the ratio η_u/η_s. The resulting values, η_x, are shown in figure 4.3. For small values of Δ the correction was large. The significance of this correction was tested as follows:

The results of the statistical survey shown in Fig. 4.2 would be consistent with a levelling off at high momenta, as was pointed out, among others, by the authors of the survey.
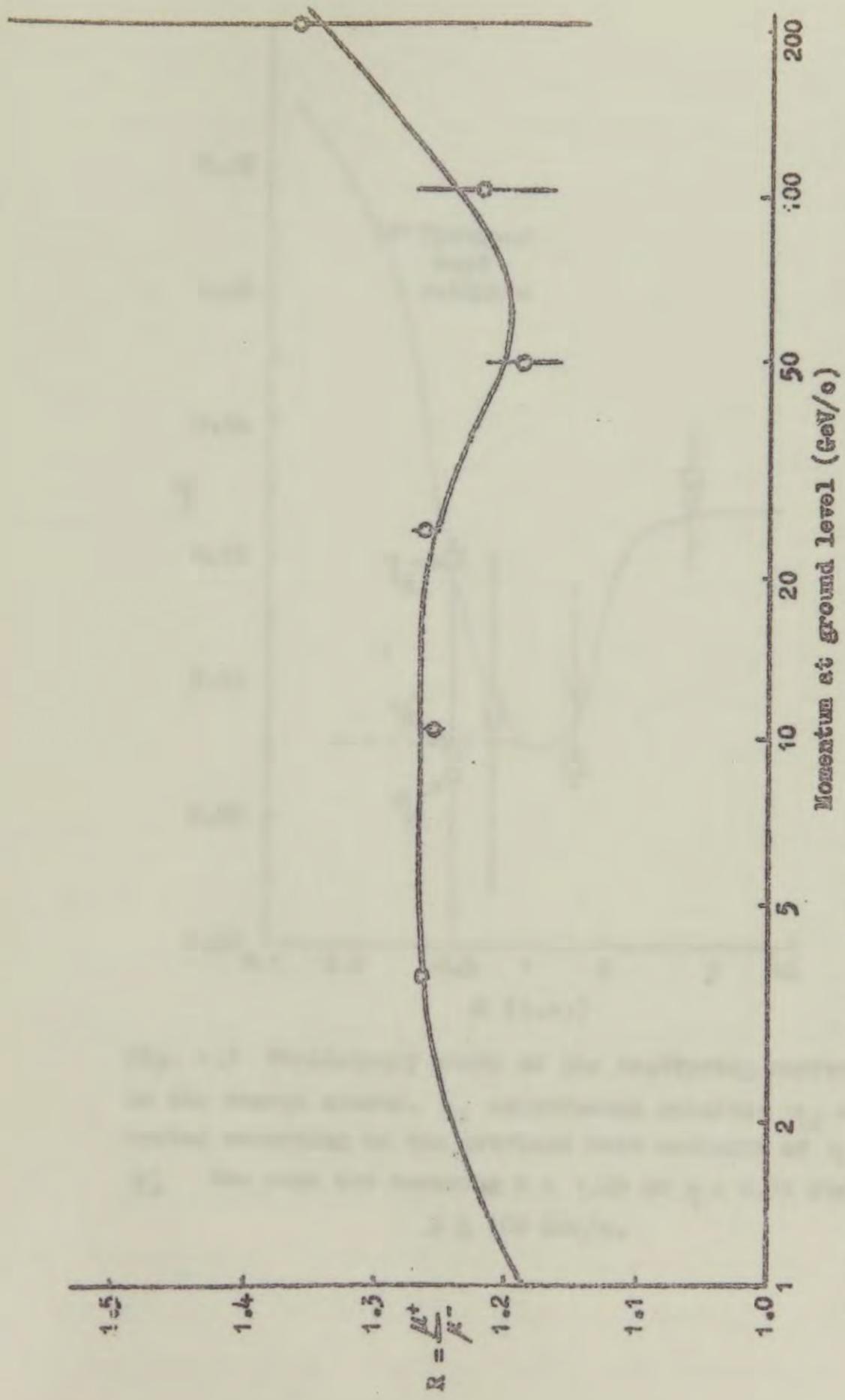
Fig. 4.2 The best estimate of the charge ratio R according to the measurements prior to 1963. The points are from the survey of MacKeown et al. (1963). See also the surveys of Ashton et al. (1963) and of Fowler and Wolfendale (1961).
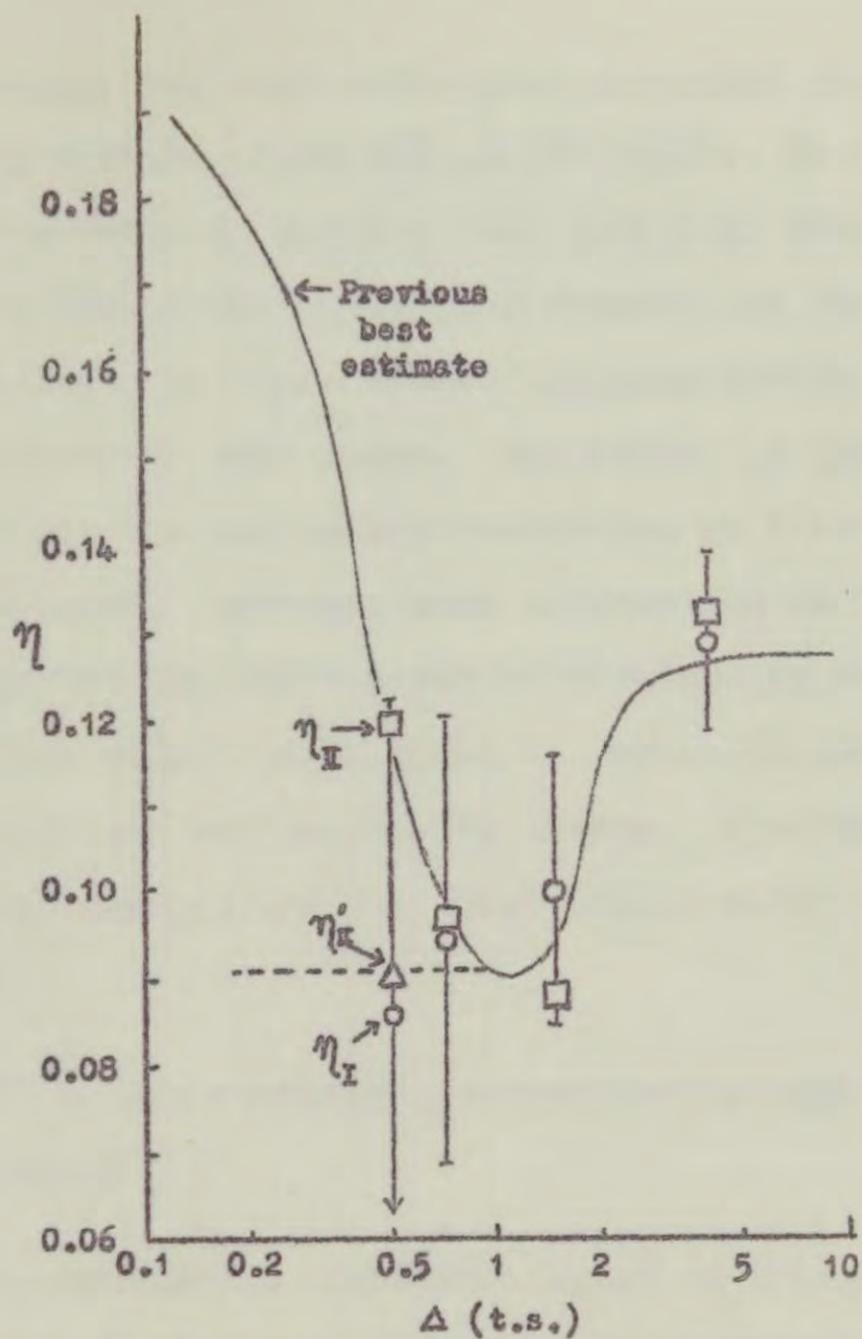
Fig. 4.3 Preliminary study on the scattering correction
to the charge excess. η_I uncorrected results; η_{II} cor-
rected according to the previous best estimate of η ;
η'_{II} the same but assuming R = 1.20 or η = 0.91 for
p $\gtrsim$ 100 GeV/c.

Accordingly, the same correction procedure was repeated
assuming that R = 1.20 for p ≳ 100 GeV/c. In this case,
the corrected R at 0.5 t.s. was just 1.2. Thus the corrected
result followed the value of R assumed for the correction
calculation. In other words, the sensitivity of the appara-
tus was poor in that range. The method of using previous
results for the scattering correction of R at high momenta
was abandoned. However, some information on the charge
ratio for p > 100 GeV/c might be obtained by means of a
correction method which would be based only on the observed
Δ-distribution and scattering theory. Obviously, an exact
error calculation for the final result would then be very
important.

4.2.6 The scattering correction by independent itera-
tion methods

The scattering correction based on a comparison spectrum
(section 4.2.4) may involve iteration, but the result remains
dependent on the comparison spectrum, the shape of which is
thought to be more or less known. The expression "independent
iteration methods" means here methods which are independent
of assumptions on the shape of the distribution which is to be
determined. Brooke (1964) used a correction method of the
independent kind. His procedure consisted of the following

stages:

a) The effect of scattering on the observed Δ-distribution
    was calculated, using the normal practice explained in
    section 4.2.4.

b) The ratio of the original height of the distribution
    to the scattered height was found as a function of Δ.

c) The observed distribution was multiplied by the
    factors found in b).

d) The effect of scattering on the distribution given
    by c) was calculated and the ratio of the heights
    before and after scattering found as a function of Δ.

e) The observed distribution was multiplied by the
    factors found in d).

f) Operations d) and e) were repeated until the ratios of
    unscattered to scattered heights reached limiting
    values.

It should be pointed out that this procedure does involve
the assumption that the distribution does not become negative
anywhere, but this is obviously justified.

It was decided to apply Brooke's method to the present
experiment, although it did not offer good possibilities for
the error calculation. In the application, a complication
arose from the fact that the observed Δ-distribution ended
at $|\Delta| = 8.15$ t.s., but yet a lot of muons were known to

scatter from above the limit (from low momenta) into the range of the experiment. Moreover, the statistics of the observed distribution were insufficient much below the limit. For the purpose of estimating the scattering contribution of the low-momentum muons, it was decided to use the OWP spectrum and the previous best estimate of R (Fig. 4.2) in the range $|\Delta| \geqslant 2$ t.s., ($p \leqslant 29$ GeV/c) where the present experiment could not be expected to improve significantly the existing statistics. In other words, the distribution in the range $|\Delta| < 2$ t.s. was to be determined, and the range $2 \leqslant |\Delta| < 8.15$ t.s. was only used for normalization purposes.

The first attempt on these lines involved the determination of the efficiency E according to the Δ-distribution in the range $2 \leqslant |\Delta| < 8.15$ t.s. The distribution in the range $|\Delta| < 2$ t.s. was then normalized accordingly. This means that the first trial distribution consisted of an unscattered distribution above 2 t.s. and of a scattered distribution, below 2 t.s., both referring to the same E. In the range $|\Delta| < 2$ t.s. the cell width was chosen as small as possible, i.e. 0.1 t.s. as used in the projection data (section 3.4.2). The iteration was performed with a computer (Elliott 803), requiring preliminary check results when the changes in the correction factors were less than 10%. The computation did

not produce any results in a reasonable time (22 iteration
cycles). This was thought to be due to the fact that the
initial trial distribution was not smooth enough.

In the second attempt, statistical fluctuations in
the observed distribution were reduced by combining cells
in the range $|\Delta| < 2$ t.s. as far as the magnitude of σ
permitted. Further, the discontinuity of the previous
distribution at 2 t.s. was removed by normalizing the
scattered distribution to join to the unscattered one,
although the value of E was then different in the two cases.
In order to avoid normalization errors which might arise
during the iteration, the unscattered distribution was always
renormalized between the iteration cycles. The computer was
arranged to print the result after every cycle. The results
of the computation showed that the main part of the scatter-
ing effect was removed by the first two or three cycles.
The following cycles took more and more into account the fine
structure of the observed distribution, which was largely due
to the statistical fluctuations. It turned out that in the
unscattered distribution the fluctuations appeared enormously
amplified. During the second, third, and fourth cycles, the
results changed significantly all the time and so the selec-
tion of the best result was inevitably arbitrary.

In the third attempt, the charge excess was omitted for

a moment in order to determine the momentum spectrum only. Then $N(+\Delta)$ and $N(-\Delta)$ could be replaced by $\frac{1}{2}[N(+\Delta) + N(-\Delta)]$, and an improvement in the statistics should be gained. Repeating the computation showed some improvement, but the arbitrariness of the result was still present.

In the fourth attempt, the observed distribution was first smoothed graphically. It turned out that a large fluctuation still grew up during the iteration. This was probably induced by a comparatively sharp bend in the observed distribution, which apparently should have been smoothed more boldly. In any case, this smoothing method turned out to be more arbitrary than the preceding attempts.

It is perhaps worth mentioning that, although the momentum spectrum could not be properly determined, the results of the different attempts appeared in general to be in the environment of the OWP spectrum. No sensible results could be obtained for the charge excess. Because of these unsatisfactory results, the iteration method was abandoned. The reason for the failure of this method becomes understandable in the analytical study in section 4.2.8.

4.2.7 The scattering correction by curve fitting

The usual curve fitting involves the choice of an analytical expression for the measured quantity. In the present case the shape of the Δ-distribution ought to be restricted to some analytical form. This procedure undeniably disagrees with the original purpose mentioned in section 4.2.5. However, the curve fitting has been very successful in the research into various momentum spectra, especially the fitting with different power expressions. Therefore it was decided to study briefly that line, too. However, the methodological error was thought to be too large for the study of the charge excess, and so only the total spectrum $i(\Delta)$ was considered.

The following expressions were tried:

$$i_I(\Delta) = a\,\Delta^c + b\Delta , \qquad\qquad 4.7$$

$$i_{II}(\Delta) = a\,\Delta^3 + b\Delta^2 + c\,\Delta , \qquad\qquad 4.8$$

$$i_{III}(\Delta) = c\,\Delta^{a\,ln\,\Delta\,+\,b} \qquad\qquad 4.9$$

where a, b, and c were parameters. The fitting was performed only in the range $|\Delta| < 2$ t.s. At the limit the curve should join smoothly to the OWP spectrum. Thus, the following initial conditions were set:

$$i(2 \text{ t.s.}) = i_{owp}(2 \text{ t.s.}) \qquad\qquad 4.10$$

$$\left[\frac{di}{d\Delta}\right]_{2 \text{ t.s.}} = \left[\frac{di_{owp}}{d\Delta}\right]_{2 \text{ t.s.}}$$

which left one adjustable parameter. A set of possible

values was given to the parameter. The scattering calcula-
tion was performed in the usual way by means of the
Elliott 803. By comparing the scattered spectrum and the
observed one, χ^2 was evaluated for each case. The values
of χ^2 were plotted against the parameter values, and the
minimum was determined graphically.

The results of these calculations are summarized in
table 4.4. The spectra i_I and i_{II} are practically identical.
Near the origin these curves behave as $K\Delta$. Thus, they
represent the kp^{-3} spectrum considered by Hayman and
Wolfendale (1962). The level of significance is rather
high for the spectra i_I and i_{II}. For i_{III}, the level is
also still reasonable. The spectrum i_{II} is considered further
in section 4.3.2.

Table 4.4 Summary of the results from the curve fitting

Curve	Adjusted parameter	Minimum of χ^2	Significance level (appr.)
i_I	c = 4.0	7.8	50%
i_{II}	a = -0.45	7.8	50%
i_{III}	a = -0.30	13.4	10%

4.2.8 The scattering correction according to the
theory of integral equations

The equation 4.4. can be immediately modified, by
changing the limits of integration, to apply to the

determination of the charge excess, i.e.

$$N(\Delta) = \int_{-\infty}^{\infty} i(\Delta_t)\sigma^{-1}\varphi\left[(\Delta - \Delta_t)\sigma^{-1}\right]d\Delta_t \qquad 4.11$$

where now $i(\Delta_t) \equiv i_+(\Delta_t)$ for $\Delta_t > 0$ and vice versa. The
determination of the unscattered spectrum requires the
solution of this integral equation in the range $|\Delta_t| < 2$ t.s.
The scattering from above 2 t.s. is calculated as before
(section 4.2.5).

Several methods of solution are known for this kind
of integral equation (see e.g. Kopal, 1961). The most
direct one is the so-called algebraic method. This involves
first the replacing of the integral by a sum according to
the well-known quadrature formulae:

$$N(\Delta) = \sum_{n} i(\Delta_n)\sigma^{-1}\varphi\,\delta_n \qquad 4.12$$

where δ_n is the cell width. In more sophisticated quadratures,
a weight factor H_n would be included in the terms. By insert-
ing the experimental values of $N(\Delta)$ into equation 4.12, a
system of linear equations is obtained where the values of
$i(\Delta_n)$ are the unknown variables. If n is set equal to the
number of the experimental values, m, the values $i(\Delta_n)$ can
be calculated algebraically. If $n \neq m$, $i(\Delta_n)$ can be determined
by a fitting calculation. Furthermore, when the fitting
method is used, certain extra requirements could be set for
the function $i(\Delta)$. In all cases, formulae for the statisti-
cal errors of $i(\Delta_n)$ may be conveniently derived in terms of

matrix notation.

The first attempt on this line consisted of the algebraic solution with no extra requirements. The Elliot 803 computer was used for the calculations. The cell system was the same as in the last iteration calculations, and so the number of the equations was 17. It was found that every second value of $i(\Delta_n)$ became negative. This fact was checked by using altogether three different programmes for the relevant matrix computations. Later, an independent confirmation was obtained from the cosmic ray spectrograph group of the University of Nottingham, where the same correction procedure had been attempted and negative intensities had been obtained (private communication from Baber, 1965). In the present work, the standard deviations of $i(\Delta_n)$, σ_n, were also computed. These were in every case greater than $|i(\Delta_n)|$ proper and so the values of $i(\Delta_n)$ were obviously useless. The large fluctuation of the results of this method is caused by the fact that the equation system is ill-conditioned (see e.g. Hartree, 1964 p.168). Consequently the Poissonian fluctuations in the observed histogram are enormously amplified.

The second attempt was a fitting calculation with the extra requirement that $i(\Delta_n)$ should not be negative. This calculation was performed so that the values of $i(\Delta_n)$ which

became negative in the algebraic solution, were fixed
to zero, and the remaining 9 values were fitted according
to the observed $N(\Delta)$. This procedure presumes that χ^2
is a rather smooth function of the parameters. The result-
ing values of $i(\Delta_n)$ and σ_n were now slightly more reasonable,
justifying the continuation of this line of study.

The third attempt was similar to the preceding one
except that the negative values of $i(\Delta_n)$ were required to
equal the mean of the adjacent values on each side. In a
way, this procedure was a method to join adjacent cells
independently of the requirement set by the standard devia-
tion of Δ (section 4.2.4). In this calculation, however,
some of the fitted values became negative.

The fourth attempt was again similar to the previous
ones, but here the values of $i(\Delta_n)$ which became negative
in the algebraic solution were required to equal the adjacent
value on the side of higher momentum. The results were
comparatively reasonable. They are shown in table 4.4
According to these results, σ is seriously large.

Table 4.4   The unscattered Δ-distribution calculated

according to the theory of integral equations

Δ (t.s.)	i(Δ) (arbitrary units)	σ
-1.95	2059	743
-1.25	2031	465
-0. 7	1094	304
-0. 3	189	378
0	193	371
0. 3	559	410
0. 7	1059	336
1.25	3064	523
1.75	2052	823

The fifth attempt was similar to the fourth one, but
here the cell system was varied. Altogether 9 trials were
made by changing the widths of the cells of the preceding
case. It was found that the result was very sensitive to
the choice of the cell system. A seemingly small change
might make some intensities negative. This fact emphasizes
the significance of the large values of σ in table 4.4.
One further trial was performed with the number of cells
increased to 13, all cells having width 0.3 t.s. The result
revealed negative intensities again. Because of the dis-
couraging results, these attempts were ceased.

The following conclusion can be drawn of the analysis
of this section. The present determination of the deflection
distribution of muons should be regarded as an indirect
experiment. The result and the estimate of its standard

deviation depend decisively on the assumed degree of smoothness of the distribution. A seemingly reasonable result may be unreliable in the sense that a relatively small change in the cell division can give rise to negative intensities.

4.2.9 The mathematical problem involved in scattering calculations

According to the preceding considerations, the scattering correction of the present experiment would require a fitting calculation in which $i(\Delta)$ would remain positive and somehow smooth but would not be bound to any analytical expression. To suit the usual applications, $i(\Delta)$ should be represented by a set of experimental points with error lines preferably only in the dimension of $i(\Delta)$. Furthermore, the points should be given with such separations that their convariances would be negligible (see e.g. Cramér, 1946, p. 295). A more detailed study would probably lead to still further requirements.

This kind of situation seems to arise rather frequently in physics when a previously unknown distribution is determined by an indirect experiment. However, within the writer's experience the present statistical theories do

not deal with this problem in the general form. The
problem is therefore considered here a little further.

It was found in the preceding section that the require-
ment $i(\Delta) \geq 0$ can, to a first approximation, be taken into
account by fixing to zero the values of $i(\Delta)$ which tend to
become negative. If χ^2 is an unsmooth function of the para-
meters, some iteration of the fitting calculations would
be needed. The same procedure could certainly be performed
by some other methods, too. In fact, according to the theory
of the extreme value problems in bounded regions, every
boundary of the allowed region should be studied separately.

The requirement of smoothness can be expressed by
demanding that the higher tabular differences, or finite
differences, should be small (see e.g. Hartree, 1964, p. 272).
A well-known difficulty is that of distinguishing between a
statistical deviation and a genuine variation. This point
has been profoundly considered in connection with two statis-
tical analyses which are closely related to the present
problem. Firstly, if the experiment is not indirect, the
statistical Fourier analysis offers a fairly efficient
method for the detection of the statistical deviations in
a distribution of unknown shape. Secondly, if the shape of

the distribution is known so that it can be represented
by an analytical expression with parameters, the χ^2-analysis
indicates roughly whether the deviations can be regarded as
accidental, i.e. whether the number of parameters is reason-
able.

A possible approach to the present problem is suggested
below. This approach has not been investigated in any
detail but serves to fix some ideas in a brief form.

The distribution $f(x)$ in question is treated as a histo-
gram. The heights of the columns, $h(x_n)$, are regarded as
independent variables which should be fitted according to the
observations (cf. section 4.2.8). The differences between
adjacent columns are denoted by $\delta_1(x)$. The higher tabular
differences are $\delta_2(x)$, $\delta_3(x)$, etc. The actual variables
$h(x_n)$ can be expressed as sums, for example, of $\delta_2(x)$,
provided one of the values $h(x_n)$ and one of values $\delta_1(x)$
are given. So the differences δ_ν can be used as the adjust-
able parameters together with one $h(x_n)$ and one δ of each
set of differences of lower degree than ν. The observed
quantity y_i is theoretically a function of $h(x_n)$, $F_i(h(x_n))$.
The usual fitting calculation finds the minimum for

$$\chi^2 = \sum_{i=1}^{N} w_i \, v_i^2 \qquad\qquad 4.13$$

where $v_i = y_i - F_i (h(x_n))$ and w_i is the weight. The requirement of smoothness could be introduced here by replacing x^2 with the quantity $x^2 + \omega^2$ where ω^2 is a measure of oscillation or unsmoothness:

$$\omega^2 = \sum_{i=1}^{N} w_i' \, \delta_{\nu i}^2 .$$ 4.14

The new weight function w_i' should be estimated according to the 'a priori' - probability of the unsmoothness. This probability function would be based only on a hypothesis, accepted beforehand on theorectical grounds. The ratio between Σw_i and $\Sigma w_i'$ determines the effectiveness of the hypothetical requirements. In most applications, the choice of w_i' would be subjective. This is characteristic for an indirect determination of a distribution. The advantage of the present method is that it would state the necessary extra requirement of smoothness in an explicit way and would not be more arbitrary than is inevitable.

The detailed study of the mathematical problem outlined in this section was not undertaken, since it could not be done within the bounds of the present work.

4.3. The final results of the experiment

4.3.1 The charge excess

No reliable scattering correction was found for the

distribution $N(\Delta)$ when the positive and negative muons were kept separate. It was therefore decided to apply a correction to Δ and also show the statistical uncertainty in that dimension.

The charge excess or charge ratio was given by the first approximation (section 3.6). The effective Δ of a cell was taken to be the median of the distribution $f(\bar{\Delta}, \Delta_t)$ where $\bar{\Delta}$ is the centre of the cell (section 4.2.4). The correction for the effect due to those muons which scatter from a positive Δ_t to a negative $\bar{\Delta}$ or vice versa, is ignored because the charge ratio from the track-simulator measurements shows that the effect is small compared with statistical errors. The resulting points are shown in Fig.5.1. The horizontal uncertainty is shown by the quartiles of $f(\bar{\Delta}, \Delta_t)$, but they should not, of course, be regarded as usual errors. According to the definition of quartiles, one half of the muons in a particular cell have a momentum within the quartile lines. It should be pointed out that any possible variation in the charge ratio appears in the present results attenuated by the scattering.

4.3.2 The momentum spectrum

In the case of the momentum spectrum, the scattering calculation based on the previous best estimate, the OWP spectrum, was accepted (section 4.2.4). Because of the

insensitivity of the experiment at high momenta
(section 4.2.5), a lower limit of 0.5 t.s. was chosen
for Δ. The usage of the integral spectrum was adopted
in order to get at least some gross information from
below 0.5 t.s. The resulting spectrum is shown in table
4.5. The observed numbers of muons are also given in the
table.

The statistical error σ_{stat} given in table 4.5. is the
Poissonian error. The standard error in the smoothed B(Δ),
σ_{bias} , is estimated from Fig. A4.1. The standard error
σ_{field} due to the inaccuracy of the average magnetic field
$\bar{B}$ (section 3.2) is converted in the dimension of $I(>p)$ to
make it analogous to the others. The total standard devia-
tion σ_{tot} was calculated by quadratic addition. To allow
for other possible error sources at high momenta, the values
of σ_{tot} at 116 GeV/c have been increased by about two units.
It should be pointed out that the values of σ_{field} are corre-
lated with each other. Also, the values of σ_{bias} depend upon
each other to some extent. Thus the values of σ_{tot} must not
be regarded as independent errors.

For the sake of comparison, the best result from the
curve fitting (section 4.2.7) is also presented (Fig. 5.2).
It does not differ much from the one accepted before.

Table 4.5 The integral momentum spectrum I($>$p) and
its standard deviation σ_{tot} , due to methodological and
statistical errors

Δ (t.s.)	p (GeV/c)	N($<\Delta$) (muons)	I (cm^{-2} sec^{-1} ster^{-1})
8.15	7.7	19235	1.06×10^{-3}
2	29.6	7711	1.29×10^{-4}
1	58.2	2703	$3.19 \times 10.^{-5}$
0.5	116	906	8.24×10^{-6}

p (GeV/c)	$\dfrac{I(>p)}{I_{owp}}$	σ_{stat} (%)	σ_{bias} (%)	σ_{field} (%)	σ_{tot} (%)
7.7	1	0.7	1	3.4	3.6
29.6	0.97	1.1	$+3 \atop -2$	4.5	5
58.2	0.91	1.9	$\pm9 \atop -3$	5.6	$+11 \atop -7$
116	0.96	3.3	$+17 \atop -4$	5.8	$+20 \atop -10$

CHAPTER 5

COMPARISON WITH THE RESULTS OF OTHER WORKERS

5.1 The charge excess

It is well-known that the absorption and decay probability of muons in the atmosphere does not change very much in the zenith angle range $\theta \lesssim 75^{\circ}$ (e.g. Hovi and Aurela, 1961; Ashton and Wolfendale, 1963). Accordingly, Ashton et al. (1964) have combined the results on the charge ratio for $\theta < 75^{\circ}$. The recent results of Rastin et al. (1965) are now included in the combination. As in their case $\theta = 0^{\circ}$, the energy at production is taken to be 2 GeV greater than at ground level. The results are shown in table 5.1.

Table 5.1 The weighted mean of the charge ratio R at
zenith angles $\theta < 75^{\circ}$ from previous measurements

$E_{\mu\,prod}$ (GeV)	Number of points	$\langle E_{\mu} \rangle_{prod}$ (GeV)	R
E < 3	9	2.72	1.170 ± 0.009
3 ≤ E < 5	10	3.90	1.215 ± 0.007
5 ≤ E < 10	21	5.78	1.264 ± 0.003
10 ≤ E < 20	21	12.4	1.250 ± 0.006
20 ≤ E < 40	19	26.0	1.258 ± 0.010
40 ≤ E < 80	6	53.5	1.164 ± 0.050
80 ≤ E < 160	6	99.9	1.233 ± 0.086
160 ≤ E	3	248	1.421 ± 0.223

Fig. 5.1 presents the comparison between the previous and the present results. The agreement is very good. In particular, the present results exhibit again slight indications of a minimum at about 50 GeV/c and of a rise above the average level towards the high momenta. It should be pointed out, however, that this variation of R with p is still statistically insignificant.

Next, the present results are also included in the world survey. The results for $E_{\mu prod} > 10$ GeV are shown in table 5.2. The low energy points do not change.

Bearing in mind the question of the kaon production (Chapter 1), the results can be compared with the results obtained at large zenith angles. An up-to-date survey of those measurements has recently been presented by MacKeown et al. (1965 a), and their results are also shown in table 5.2. When the results at 182 and 430 GeV are combined (weighting according to $1/\sigma_R^2$), the mean energies are satis-factorily equal with the energies obtained in the case $\theta < 75^{o}$. Then following MacKeown et al., the ratio $R(\theta > 75^{o})/R(\theta < 75^{o})$ is calculated according to these data. The quantity $\bar{E}_{\mu prod}$ in table 5.2 is the arithmetic mean of the two relevant mean energies. It is seen that the statistics are still insufficient for ascertaining the possible difference between the compared ratios. However,
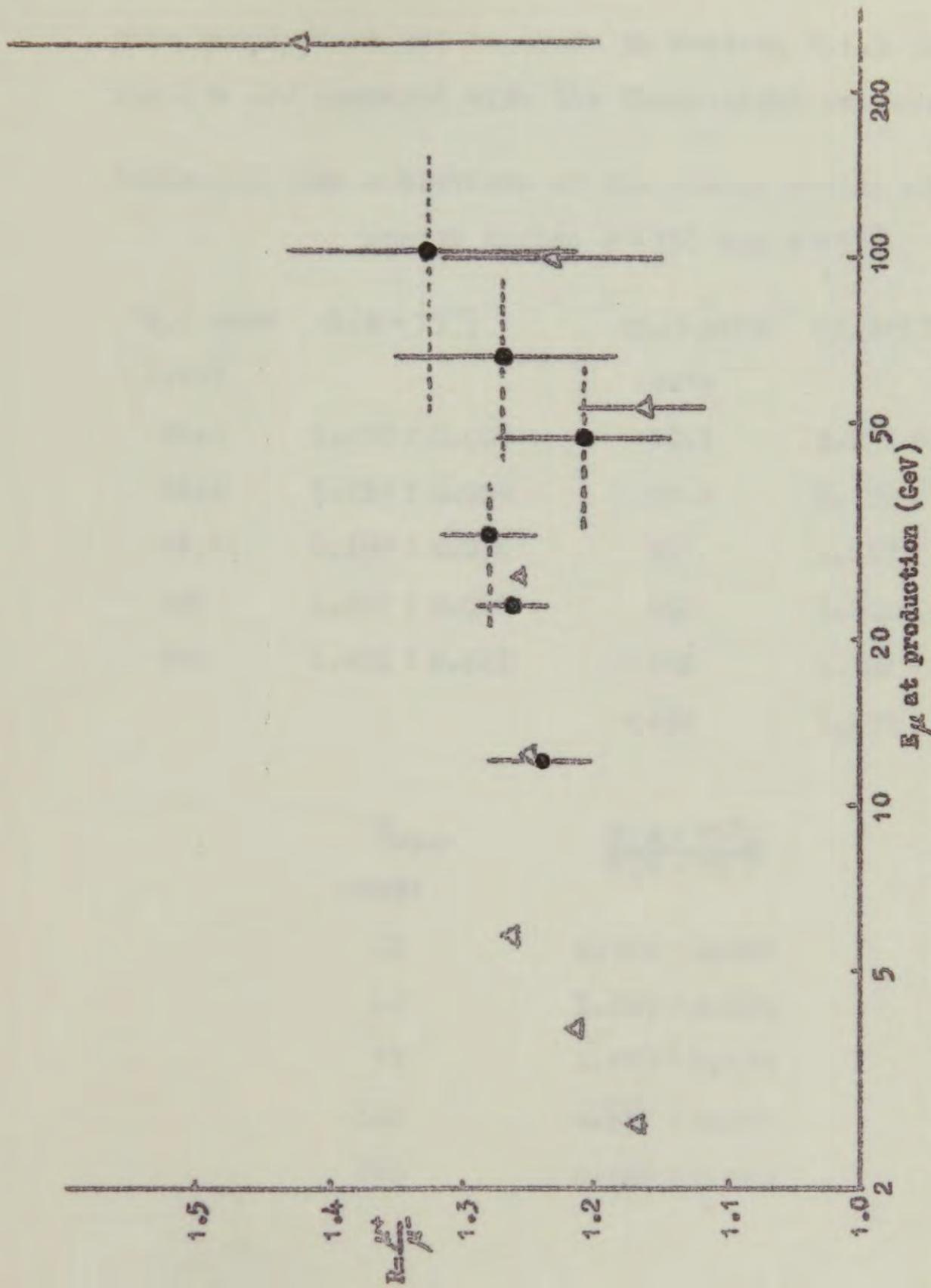
Fig. 5.1 Comparison of the charge ratio from the present work (solid points) with the best estimate from previous workers (in the near vertical direction).

some conclusions can be drawn in section 6.4.3 when these results are compared with the theoretical expectations.

Table 5.2 The comparison of the charge ratios at the zenith angles $\theta < 75^{\circ}$ and $\theta > 75^{\circ}$

$\langle E_\mu \rangle$ prod (GeV)	$R(\theta < 75^{\circ})$	$\langle E_\mu \rangle$ prod (GeV)	$R(\theta > 75^{\circ})$
12.5	1.250 ± 0.006	18.5	1.235 ± 0.120
26.4	1.259 ± 0.009	29.1	1.270 ± 0.023
54.8	1.195 ± 0.036	55	1.227 ± 0.026
102	1.267 ± 0.068	102	1.212 ± 0.038
248	1.421 ± 0.223	182	1.192 ± 0.068
		~ 430	1.237 ± 0.18

$\bar{E}_{\mu\,prod}$ (GeV)	$\dfrac{R(\theta > 75^{\circ})}{R(\theta < 75^{\circ})}$
15	0.988 ± 0.096
28	1.009 ± 0.020
55	1.027 ± 0.038
102	0.957 ± 0.060
230	0.844 ± 0.140

5.2 The momentum spectrum

In deriving the OWP spectrum mentioned earlier, Osborne et al. (1964) resolved the bulk of the discrepancy between the muon spectra obtained from the gamma cascade measurements and from the burst measurements, except for the measurements of the Moscow Group (Chapter 1). The OWP spectrum is therefore considered to be the best estimate from the previous experiments. The present spectrum is compared with it in table 4.5 and in Fig. 5.2. In general, agreement is found. Concerning the scattering correction, this agreement indicates that the OWP spectrum was a good comparison spectrum so that no iteration was necessary. The scattering correction by curve fitting gives a quite similar spectrum.

In the region 50 - 100 GeV/c there is an indication that I_{owp} might be too high by a few per cent. However, a discrepancy of the magnitude would also originate from the inaccuracy of the present work. When considering this discrepancy, it should be remembered that a part of the bias data of Palmer have also been used for the correction of the OWP spectrum. Nevertheless, the bias data used in present work are in the range p > 50 GeV/c mainly based on independent additional statistics, corresponding to the knock-on electrons produced in the magnet plug. On grounds of the large values
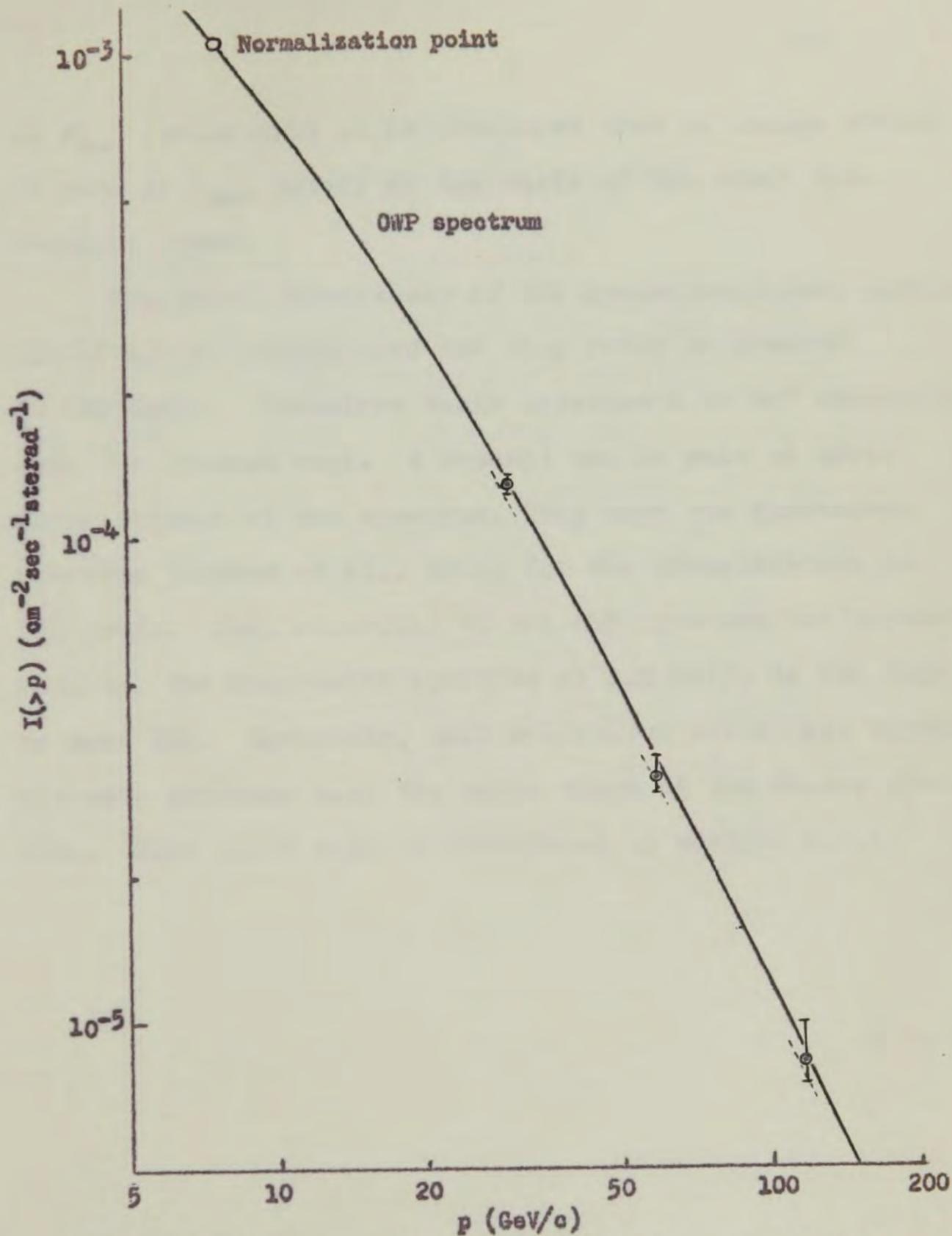
Fig. 5.2 Comparison of the present results on the integral
spectrum with the OwP spectrum (Osborne et al., 1964). The small
dashed lines show the spectrum $\int i_{II} dA$ considered in section 4.2.7.

of σ_{tot} (table 4.5) it is concluded that no change should be made to I_{OWP} solely on the basis of the small discrepancy found.

The burst experiments of the Moscow Group were carried out 40 m w.e. underground and they refer to momenta p > 100 GeV/c. Therefore their experiment is not comparable with the present work. A comment can be made on their normalization of the spectrum. They used the Manchester spectrum (Holmes et al., 1961) for the normalization at 100 GeV/c. Now, according to the OWP spectrum and present results, the Manchester spectrum at 100 GeV/c is too high by some 20%. Obviously, this error does not at all explain the main problem, i.e. the small slope of the Moscow spectrum. This point will be considered in section 6.2.4.

CHAPTER 6

INTERPRETATION OF THE RESULTS

6.1 Introduction

The interpretation of the charge excess and momentum
spectrum of muons involves three sets of parameters: (i)
the energy spectrum and charge composition of the primary
cosmic-ray nuclei, (ii) the characteristics of the propa-
gation of the primary and secondary particles in the atmos-
phere, and (iii) the characteristics of nucleon –
air-nucleus collisions in the energy region 100 GeV – 100
TeV. Previous experiments have given a satisfactory quanti-
tative description of the primary radiation and the propa-
gation of the various particles in the atmosphere. Accord-
ingly the interest in this interpretation is mainly in the
nuclear collisions, where even the qualitative knowledge is
unsatisfactory. Several collision models are at hand, and
the models which are of interest in the present application
are described briefly in the following review.

6.2 Models for high-energy nuclear interactions

6.2.1 The composite empirical model

Because of the uncertainty of the hypotheses concerning
the nature of the nuclear interactions, the characteristics

of nucleon-nucleon collisions are best given by certain empirical expressions obtained from different experiments. These expressions are here considered to form a composite empirical model in order to treat them in conformity with theoretical models. The empirical model has been extensively developed and used by the cosmic ray group of Durham University (e.g. Wolfendale, 1963; Brooke et al., 1964; MacKeown et al., 1965 a) in the interpretation of the muon spectrum and charge excess.

To begin with, the characteristics of the pionization process are considered. Cocconi et al. (1961) have put forward an empirical relation (to be referred to as the CKP relation) to account for the observed energy spectrum of pions from the interactions of protons with light elements at accelerator energies ($\leqslant 30$ GeV). They find the following expression for the mean number of pions of one sign in the forward direction in the centre-of-mass system (C system):

$$\langle N(E_\pi)\rangle \, dE_\pi = (A/T)\exp(-E_\pi/T)dE_\pi \qquad\qquad 6.1$$

where E_π is the energy of the pion in the laboratory system (L system), A is the mean multiplicity of pions of one sign emitted in the forward direction in the C system, and T is

the mean pion energy. Bowler et al. (1962) have also
found some supporting evidence for this relation from
high-energy jets. The relationship between A and T is
given by equation

$$AT = K_\pi E_0/3$$

where E_0 is the primary energy and K_π is the fraction of
E_0 given to pions of all charge states. Cocconi et al.
also assume that the mean multiplicity follows the Fermi
equation $\langle n \rangle \propto E_0^{\frac{1}{4}}$ where $\langle n \rangle$ is the mean of the total number
of secondaries. Considering pions only, the following
relation is valid:

$$\langle n \rangle = 6A = cE_0^{\frac{1}{4}} .$$

The factor 6 arises when allowance is made for the three
charge states of the pions and the 50% of the pions which
are emitted in the backward direction in the C system and
are assumed to have negligible energy in the L system.
There is evidence for the validity of the quarter-power
law from a number of experiments, ranging from machine-
experiments at tens of GeV to studies with ionization calori-
meters at several hundred GeV and emulsions at energies of
about 10 TeV (summarized by Brooke et al., 1964).

Brooke et al. have introduced a simplified model in which it is assumed that pions are emitted with equal energy in the C system, half being in the forward and half in the backward direction. The corresponding energy of fast pions in the L system is taken as $K_\pi E_o/3A$. This model (to be referred to as constant-energy or CE model) is justified by the fact that the spectrum of muons has been found to be rather insensitive to the form of the energy spectrum assumed for pions generated in a nuclear collision. The CE model can be regarded as a limiting case and it has been found useful when studying the effects of varying the other parameters.

Brooke et al. have also proposed an empirical expression for the distribution in the elasticity f of nucleon - air-nucleus collisions. The experiment of Dodd et al. (1961) suggests a broad distribution and therefore the following form was accepted:

$$P(f)df = -(1+\alpha)^2 f^\alpha \ln f \ df \qquad\qquad 6.2$$

(to be referred to as BHKW distribution). The constant $\alpha = 1.43$ was found to fit the previous knowledge of the atenuation of the nucleonic component in the atmosphere. As K_π is not much less than the total inelasticity $K_t = 1 - f$, K_π must also have large fluctuations. Consequently, a

distribution of the BHKW form was accepted for $1 - K_\pi$:

$$P(K_\pi)dK_\pi = -(1+\alpha')^2 (1 - K_\pi)^{\alpha'} \ln (1 - K_{\overline{\pi}})dK_{\pi'} . \quad 6.3$$

The value $\alpha' = 3.6$ was found to fit the previous knowledge of the relation between the primary nucleon spectrum and the pion production spectrum (section 6.3.2). The distribution was compared with the experimental distribution observed by Guseva et al. (1962) using the ionization calorimeter technique and general agreement was found. There was, however, a small discrepancy in the region $0.9 < K_\pi < 1.0$ where equation 6.3 predicts practically no events but the observed distribution showed a few. This could be explained by the well-known imperfections of the particular technique used but the later observations by Babayan et al. (1963) suggest that some exceptional events with $K_\pi \approx 1$ do exist. The explanation of these events requires some other collision model (see sections 6.2.4 and 6.4.2).

MacKeown et al. (1965 a) have put forward an empirical expression for the observed distribution of the multiplicity (to be referred to as MSWW distribution). They found that the existing data are reasonably fitted by the Polya distribution

$$\sigma_n(E_0) = (\langle n \rangle^n / n!)(1 + \zeta \langle n \rangle)^{-(n + 1/\zeta)} \prod_{j=1}^{n-1}(1 + j\zeta) \qquad 6.4$$

where $\langle n \rangle = 2.7 \, E_0^{\frac{3}{4}}$ and $\zeta = \zeta(E_0) = 0.4 \, (1 - \exp(E_0/5550))$ with E_0 in GeV. This slightly underestimates the frequency of the events with $n_{\pi^\pm} = 1$ and $n_{\pi^\pm} = 2$.

Next, some characteristics of the production of particles other than pions are considered from the point of view of muon research. It is known that kaons can play an important role in muon production. Hyperons are generated relatively rarely and if they have a decay mode into muons they give only a comparatively small fraction of their energy to the muons. Therefore the contribution of hyperons to the number of muons of a given energy is negligible.

Following the observations from the accelerator experiments, the Durham group (MacKeown et al., 1965 a) has recently put forward the following model for the kaon production: The kaon production spectrum is parallel to the pion production spectrum; the abundance ratio $K^+/K^- = 4$ independent of the nature of the primary nucleon; $K^\pm/(K^0, \overline{K^0}) = 1$. (The important ratio K/π has been kept as an adjustable parameter.)

6.2.2 The isobar model

The current idea of the high-energy nucleon-nucleon collisions assumes that the nucleons emerge from the

collision as isobars which return to the ground state by emitting pions which, because of the motion of the isobars, have high energies in the L system. At the same time further pions with lower energy are produced through an independent materialization of the kinetic energy. According to a model of phenomenological origin, the material-ization produces one or more "fire-balls" which then decay into pions (e.g. Cocconi, 1958 and 1965). Recently Peters (1965) suggested a more fundamental hypothesis according to which the materialization would create one or more pairs of isobars and anti-isobars which then annihilate producing pions.

6.2.3 Peripheral collision model

The next important alternative for the production of the high-energy muons seems to be the peripheral collision model which was first considered by Narayan (1964) and later developed in a more rigorous and general form by Crossland and Fowler (1965). The model can be postulated to involve the peripheral exchange of either a pion or a K^* meson. According to unitary symmetry considerations, the latter postulate would also involve pion production via ρ meson exchange. The value obtained from the pion-exchange model

for the cross-section for production of π^+ in a proton-nucleon collision with an inelasticity $k_\pi \geq 20\%$ is about 2mb. For production of K^+ by K^* exchange with the same inelasticity limit the value is 0.5 mb. A similar cross-section is expected for the ρ meson exchange.

6.2.4 Other models

Grigorov and Shestoperov (1963) have proposed a phonomenological model in order to explain the new type of collision found in nuclear emulsions (Babayan et al., 1963) in which the inelasticity is close to unity and about 50% of the primary energy is, on average, transferred to one π^o meson. Their model is equivalent to postulating very heavy isobars and is, in fact, an 'ad hoc' speculation.

Vernov et al. (1965) suggested that the odd results of the burst experiments of the Moscow Group (cf. Chapter 1) could be explained by the possible existence of so-called "X-particles". The mass of these particles would be very great, perhaps 10 or 100 times the nucleon mass. They would be nuclear-active but, on theoretical grounds, their relative energy loss in nuclear interactions would be very small. This is again an 'ad hoc' model, but it may be related to the more fundamental theory mentioned next.

The theories of unitary symmetry suggest the possible existence of new elementary particles of rest mass greater

than a few GeV, called quarks (Gell-Mann, 1964). At this moment, quarks are only mathematical tools which have been found useful in the systematization of elementary particles (Koba, 1965). If such particles really exist, however, they could change completely the present idea of a nuclear collision.

6.3 The interpretation of the muon spectrum

6.3.1 Relation to the spectra of pions and primary nucleons

In the momentum range of the present experiment, the interpretation of the sea-level muon spectrum has been well established by previous workers (e.g. Brooke et al., 1964) and therefore it is only briefly reviewed here. The interpretation requires, in the first place, explanation of the relation of the muon spectrum, through the pion production spectrum, to the primary spectrum.

It can be assumed that pions are the sole source of muons of energy below 100 GeV. Then the muon spectrum $N_\mu(E)$ is related to the pion production spectrum $P(E_{\pi^\pm})$ by the following equation:

$$P(E_{\pi^\pm})dE_\pi = N_\mu(E_\pi/r)(1 + E_\pi/rB)D(E_\pi)(1/r)dE_\pi \qquad 6.5$$

where B = 90 GeV, $r = m_\pi/m_\mu = 1.32$ and $D(E_\pi)$ is a factor which allows for loss of muons by decay and energy loss by ionization in the atmosphere. $D(E_\pi)$ tends to unity for energies in excess of 20 GeV.

The relationship between the primary spectrum, the pion production spectrum, and the parameters of the inter-action can most easily be seen by using the constant-energy model. Assuming that the primary spectrum follows a power-law in the energy range concerned, i.e.

$$Np(Eo)dEo = b\,Eo^{-\gamma}\,dEo,$$

and that K_t and K_π are constant for each interaction and do not vary with energy, it can be shown that the predicted production spectrum is given by

$$P(E_{\pi\pm})dE_\pi = \frac{2}{1 - (1 - K_t)^{\gamma-1}}\ \frac{b}{1-\alpha}\ a^u\ \left(\frac{K_\pi}{3}\right)^v\ E_\pi^w\ dE_\pi \quad 6.6$$

where $u = (2 - \gamma)/(1 - \alpha)$, $v = (\gamma - \alpha - 1)/(1 - \alpha)$, and
$$w = (2\alpha - \gamma)/(1 - \alpha).$$

The quantities α and a are the exponent and co-efficient of the Fermi equation $A = a\,Eo^{\frac{1}{4}}$. The term $1/[1 - (1-K_t)^{\gamma-1}]$ gives the sum of the contributions from each generation, i.e. it corresponds to the sum of the pions produced by the primary nucleons, nucleons which have interacted once, twice, etc. If the CKP relation is taken for the pion energy spectrum instead of the CE approximation, it can be shown that the

pion production spectrum is given by

$$P(E_\pi t)dE_\pi = \frac{2dE_\pi}{1 - (1 - K_t)^{\gamma - 1}} \quad \frac{3a^2 b}{K_\pi} \int\limits_{3E_\pi}^{\infty} Eo^{-\gamma - \frac{1}{2}} \exp(\frac{3aE_\pi}{K_\pi Eo^{\frac{3}{4}}})dEo. \quad 6.7$$

6.3.2 Relation to the spectrum of secondary nucleons

Because of the well-known genetic relations between the secondary cosmic rays, the interpretation of the muon spectrum should also fit the observed spectra of the other secondary components. At high energies, these relations have proved useful in determining the characteristics of nuclear interactions. Wolfendale (1963) and his collaborators (Brooke et al., 1964) have considered in this way the primary spectrum $Np(E)$, the sea-level nucleon spectrum $N_n(E)$, and sea-level muon spectrum $N_\mu(E)$. Essentially, $N_n(E)$ gives information about the total inelasticity K_t in nucleon - air-nucleus collisions, and $N_\mu(E)$ gives information about K_π. In the actual analysis it turned out that the sensitivity of the various parameters and their previous measuring accuracy were such that new information was obtained both of the inelasticities and of the primary spectrum. The best estimate of the average inelasticity K_π was 35%, $K_t - K_\pi$ being 12%. The integral spectrum of the primary nucleons could be expressed with a constant exponent in the range 10 GeV - 30 TeV by the form

$$N_P(>E) = 0.87^{+0.52}_{-0.30} \; E^{-1.58} \quad cm^{-2} \, sec^{-1} \, sterad^{-1} \qquad 6.8$$

with E in units of GeV/nucleon. This analysis was based on the HPW spectrum (Hayman et al., 1963).

Recently Malholtra et al. (1965) have determined the spectrum of primary nuclei in the range 100 GeV - 600 TeV by measuring the spectra of gamma cascades at balloon altitudes. Their spectrum agrees with the spectrum given by equation 6.8 to within a few per cent, in fact much better than the error estimates would suggest. On the other hand, the direct measurements by the satellite Proton I (Grigorov et al., 1965) have resulted in a much steeper spectrum, the exponent of which changes from -1.75 at 10 GeV to -1.95 at 100 TeV (Vernov, 1965). At 100 GeV this spectrum is lower than the preceding ones by about 25%, which is still within the error estimates, but at 30 TeV it is lower by a factor of nearly 9.

A remark can be made on this question from the results of the present work. The muon spectrum in the proximity of 100 GeV is sensitive to the primary energies around 10 TeV. The present spectrum is a few per cent higher than the HPW spectrum, and thus, to a first order of approximation, the primary spectrum should be even higher than given by equation 6.8, by a few per cent. As McCusker (1965) has pointed out,

it would in general be difficult to construct a collision
model which would give the observed spectra of the secon-
dary cosmic rays if the satellite spectrum should be accep-
ted. In particular, large cross-sections would be needed
for high-energy muon production (see also Chapter 7).

6.3.3 Relation to the spectrum of gamma cascades

Osborne and Wolfendale (1964) have compared the measured
spectra of gamma cascades and muons. They predicted the muon
spectrum at sea level on the basis of all pions or all kaons
as the source of the cascades and the muons. Comparison was
made with the OWP spectrum mentioned earlier, and by inter-
polation the ratio K/π could be derived. Under the assump-
tion that the energy spectra of pions and kaons have the
same form, K/π was found to vary from 20 ± 20 % at 20 TeV
through 10^{+15}_{-10} % at 70 TeV to 40 ± 30 % at 600 TeV (mean primary
energies).

6.3.4. Relation to the muon spectra in inclined
directions

As mentioned in Chapter I, the comparison between the
muon spectra in the vertical and inclined directions should
give an estimate of K/π . Recently Ashton et al. (1965) and
MacKeown et al. (1965 b) have obtained in this way the

result $K/\pi \lesssim 0.4$ for primary energies up to 100 TeV, with
some slight evidence for an increase in the ratio at the
highest energies. This result agrees with the result
obtained by Osborne and Wolfendale (see above).

6.4 The interpretation of the charge excess

6.4.1 The dependence of the charge excess on the collision characteristics

The relationship between the charge excess of muons
at production and the different characteristics of the
nuclear collisions can be approximately represented by the
following equation (MacKeown et al., 1965):

$$\eta(E_\mu) = \frac{3}{2} D(E_\mu) \frac{\sum_n \iiint N(E_0) \sigma_n(E_0) P(K_\pi) N(E_\pi) n_\mu(E_\mu) \Delta(n, E_\pi) dE_0 dK_\pi dE_\pi}{\sum_n \iiint N(E_0) \sigma_n(E_0) P(K_\pi) N(E_\pi) n_\mu(E_\mu) dE_0 dK_\pi dE_\pi} \cdot \qquad 6.9$$

Here $D(E_\mu)$ is a dilution factor to account for the composi-
tion of the primary radiation and its varying charge composi-
tion in the atmosphere. This includes the charge excess of
the primary nucleons: $(p - n)/(p + n) = 0.74$, where p and n
are the abundances of protons and neutrons, respectively.
$N(E_0)dE_0$ is the spectrum of primary nucleons, $\sigma_n(E_0)$ is the
distribution in total multiplicity, and $p(K_\pi)dK_\pi$, $N(E_\pi)dE_\pi$
are the inelasticity and energy spectra in a collision, re-
spectively. Finally, $\Delta(n, E_\pi)$ is the charge excess per pion

having energy E_π. The equation 6.9 presumes that the charge excess comes from the first generation of pions.

6.4.2 The expected charge ratio from various collision models

MacKeown et al. (1965 a) have calculated the charge ratio R using various collision models. In the empirical model, the MSWW expression mentioned earlier was used for $\sigma_n(E_0)$. For $P(K_\pi)$, the BHKW distribution was adopted with $\langle K_\pi \rangle = 0.31$. For $N(E_\pi)$ an expression was used which when combined with $\sigma_n(E_0)$ and $P(K_\pi)$ resulted in the average distribution given by the CKP relation. A forward-backward distribution

$$f(\cos \vartheta) = \tfrac{1}{2} \delta(1 - |\cos \vartheta|)$$

has been taken where δ is the Dirac function. The primary spectrum was taken from Brooke et al. (1964) (see equation 6.8). The probability of charge exchange in a proton-air-nucleus collision was assumed to be 50%, independent of energy. Then $\Delta(n, E_\pi) = \tfrac{1}{2} n^{-1}$ at large n. It was found that R is very insensitive to $P(K_\pi)$, $N(E_\pi)$, and π-μ decay spread. The results obtained for R assuming different values for K/π are shown in Fig. 6.1. MacKeown et al. pointed out that the assumption of similar production spectra for pions and kaons and the uniform distribution of the charge excess
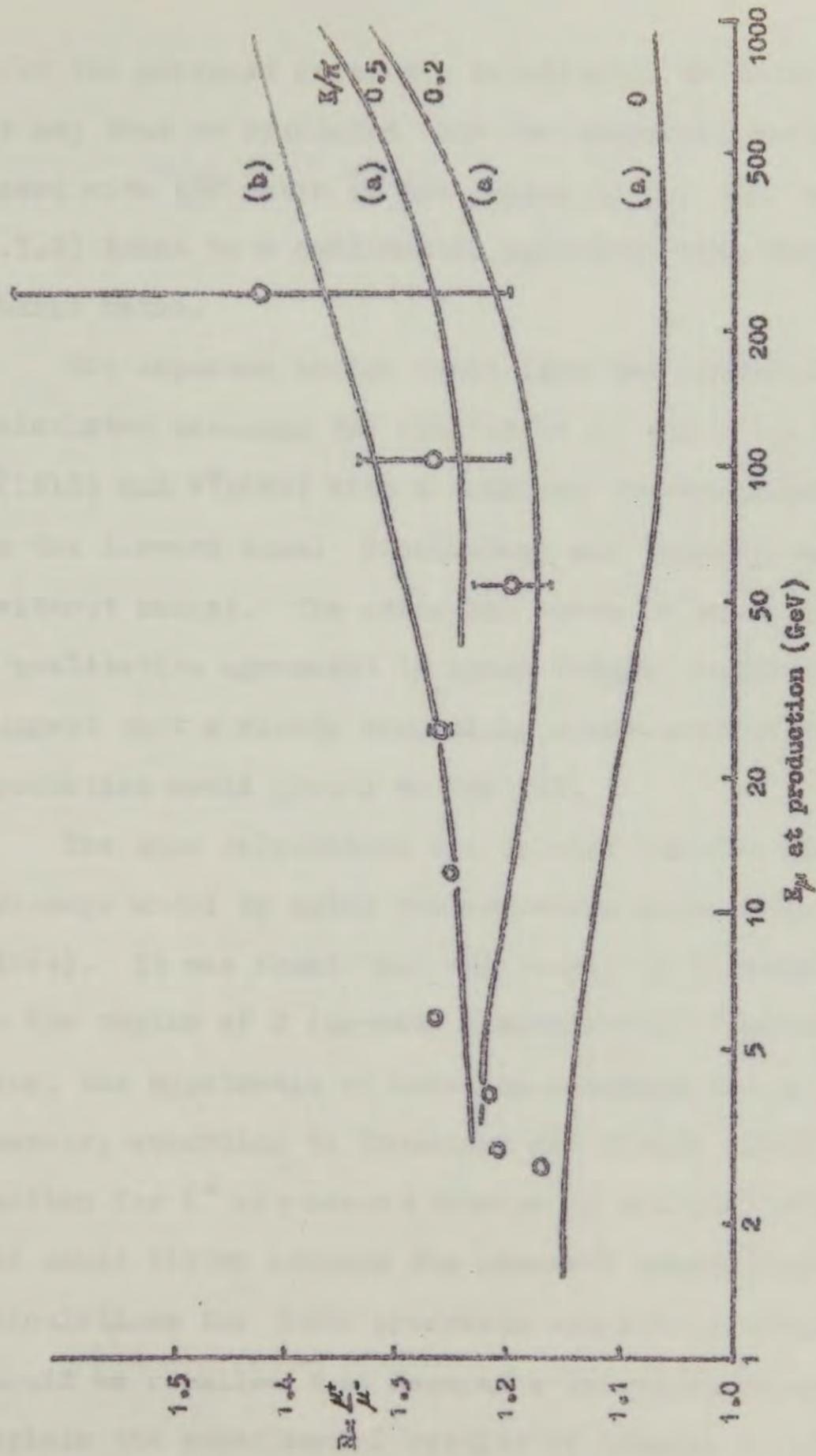
Fig. 6.1 Comparison of the best estimate of the charge ratio in the near vertical direction with theoretical expectations (MacKeown et al., 1965 a). Curveu (a) from the empirical model with different portions of kaons. Curve (b) from the isobar model including empirical pionisation.

over the produced kaons may be adjusted to some extent.
It may thus be concluded that the empirical collision
model with K/π ratio in the region of 0.2 (cf. section
6.3.3) leads to a qualitative agreement with the observed
charge ratio.

The expected charge ratio from the isobar model was
calculated assuming the excitation of the $T = \frac{1}{2}$ isobars
$N^*(1518)$ and $N^*(1688)$ with a constant cross-section of 3 mb.
in the forward cone. Pionization was included as above
(without kaons). The resulting curve is shown in Fig. 6.1.
A qualitative agreement is again found. MacKeown et al.
suggest that a slowly decreasing cross-section for the isobar
production would give a better fit.

The same calculation was carried out for the one-pion-
exchange model by using the cross-sections given by Narayan
(1964). It was found that the values of R became very high,
in the region of 2 (private communication from MacKeown).
Thus, the hypothesis of one-pion-exchange has to be rejected.
However, according to Crossland and Fowler (1965), the cross-
section for K^* or ρ meson exchange is smaller (section 6.2.3)
and could better explain the observed charge ratio. Detailed
calculations for these processes are not yet available. It
should be recalled that Narayan's calculations could also
explain the experimental results of Babayan et al., concerning

the interactions with the 'catastrophic' inelasticity (section 6.2.4). This point should also be reconsidered according to the new theory.

6.4.3 Variation of the charge ratio with zenith angle

MacKeown et al. (1965 a) have calculated the variation of the charge ratio R with zenith angle θ from the empirical model by using the values 0, 0.2, and 0.5 for the abundance ratio of kaons to pions. The curves obtained are shown in Fig. 6.2. The combined experimental data from section 5.1 are also shown.

The results of the present experiment have changed the previous statistics so that a finite kaon contribution in the charge excess has become more probable, but quantitative conclusions cannot yet be drawn. In a very approximate way it can be said that the combined data suggest a value $K/\pi \approx 0$ for $E_\mu \lesssim 80$ GeV and an increasing value up to $K/\pi \approx 0.5$ for $80 \lesssim E_\mu \lesssim 230$ GeV. This estimation agrees with the one made by Ashton et al. (1965) from the inclined muon spectra (section 6.3.4) and it is also consistent with the results of Osborne and Wolfendale (1964) based on the gamma cascade spectra (section 6.3.3).
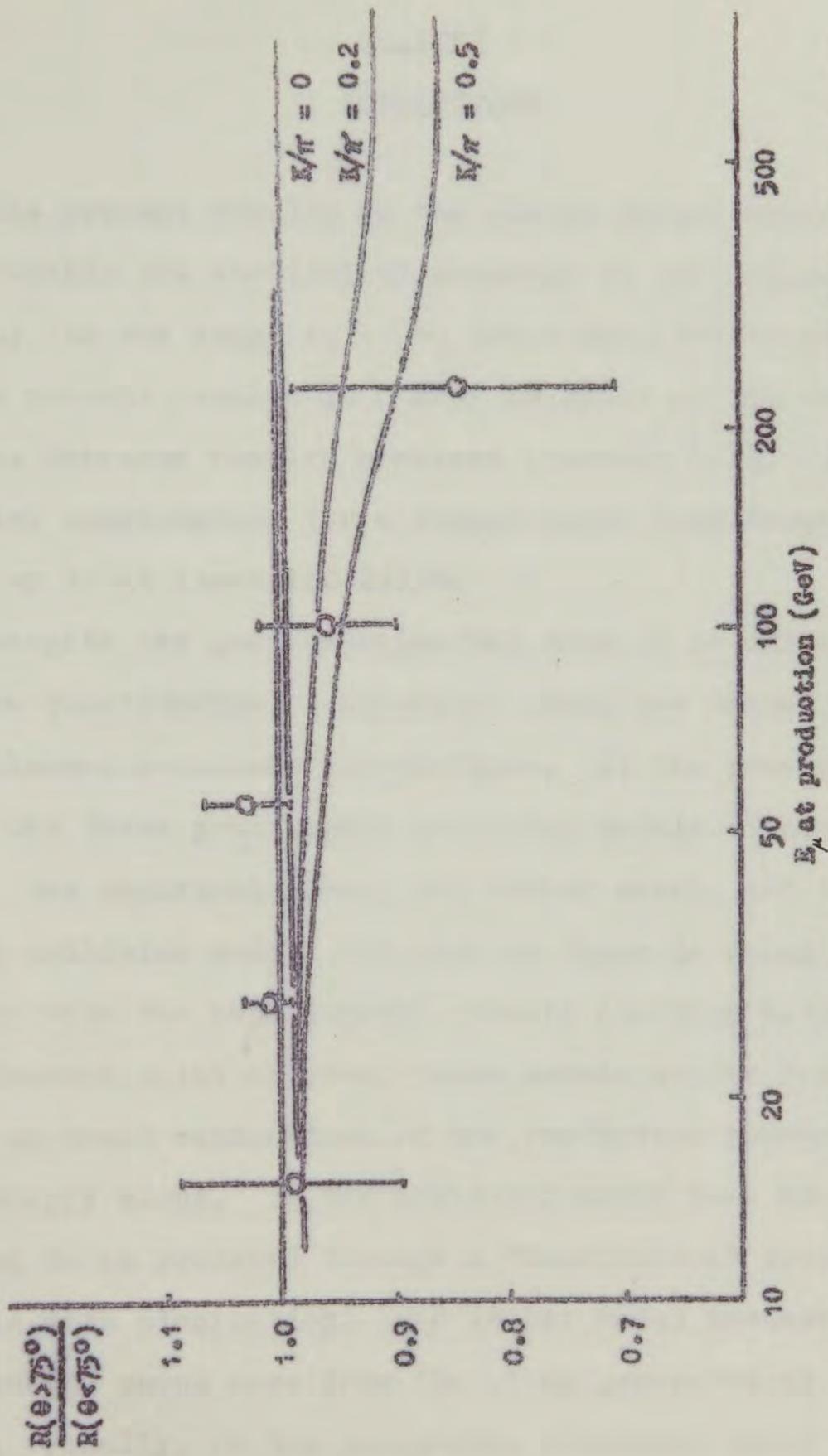
Fig. 6.2 Comparison of the experimental results on the ratio $R(\theta > 75°)/R(\theta < 75°)$ with the theoretical expectations calculated by MacKeown et al. (1965 a) from the empirical collision model with various values of K/π.

CHAPTER 7

CONCLUSIONS

The present results on the charge excess increased considerably the statistical accuracy in the high-energy region; in the range 40 - 160 GeV/c the statistical weight of the present results is nearly as great as the weight of all the previous results combined (section 5.1). They give positive confirmation for a charge ratio significantly above unity up to at least 100 GeV/c.

Despite the good experimental data it is still difficult to draw quantitative conclusions about the characteristics of nucleon-air-nucleus interactions. At the present time there are three practicable collision models at hand (section 6.2): the empirical model, the isobar model, and the peripheral collision model, and each of these is found to be consistent with the experimental results (section 6.4). From the experimental point of view, these models differ from each other in their explanation of the production mechanism of high-energy muons. In the empirical model such muons are assumed to be produced through a "kaonization" process, comparable with pionization. The isobar model assumes that the high-energy muons come from the pions generated by isobar decay. Finally, in the peripheral collision model those muons are produced via K^* or ρ exchange.

A more profound insight may follow from a recent work by Feinberg (1965). He found that according to the field theory nucleons emerge from a nuclear interaction with their fields disturbed. According to Peters (1965) this means that the nucleons are in isobar states. Now, the peripherical collision model may be regarded as the first approximation in the field-theoretical treatment of strong interactions, and it seems thus to be basically identical with the isobar model. Then the three collision models used in the interpretation of the charge excess represent only different levels of one theory. The empirical model is based only on the statistics collected of certain characteristics of the materialization in nuclear interactions. The isobar model describes the nature of the interaction in more detail, but the crucial cross-section is still experimental. In the peripheral collision model the cross-section is determined from theory. From this point of view it is significant that the empirical model and the peripheral collision model agree in suggesting a strong kaon contribution at high energies. The present isobar model seems to be deficient in this respect.

The considerations above suggest that the peripheral collision model would be most important in the interpretation of the charge excess. The cross-sections should be calculated

for different values of inelasticity by the method of
Crossland and Fowler and the results should be tested
as before by the experimental charge excess and also
by the data on the 'catastrophic' collisions (section
6.4.2). The same procedure should be possible in terms
of the isobar model if the kaon production would be incor-
porated in it. The possible explanation of the pioniza-
tion process by the annihilation of isobar pairs (section
6.2.2) would be very interesting but, concerning the charge
excess, this new explanation should not change much the
results obtained from the empirical model.

The present results on the muon spectrum confirm the
essential correctness of the OWP spectrum (Osborne et al.,
1964) (section 5.2). This fact supports the previous
interpretation of the production of the muon component of
cosmic rays and the corresponding estimation of the primary
spectrum (Brooke et al., 1964). There are, however, two
esperimental spectra which do not fit to the present scheme.
The primary spectrum measurements from the satellite Proton I
have suggested much lower intensities at high energies. The
interpretation of these results would require a new collision
model providing large cross-sections for the production
of high-energy muons (section 6.3.2). As has been pointed
out by Wolfendale (1965), it would then be

difficult to obtain the relatively low charge excess of muons observed at sea level (section 6.4.2). Obviously it would be important to repeat the direct measurements in another satellite, preferably by a different technique.

The recent burst spectrum of the Moscow Group (section 5.2), which gives a much flatter muon spectrum than reported here, also remains unexplained. None of the other recent underground experiments suggest any basic change in the present idea of the hard component of cosmic rays (see Wolfendale, 1965). Similarly the previous burst spectra on ground level and underground (Chapter 1) showed steeper slopes. Thus, that exceptional experiment also calls for a check measurement.

To return to spectrograph measurements, a few methodological remarks can be made. The new kind of plumb-line system used in the alignment of the spectrograph and the new method of measuring the field in the solid iron magnet were successful and could be useful in similar experiments. On the other hand, the Coulomb scattering in the magnet plug was found to be serious and, in fact, it prevented the study of muons with momentum much above 100 GeV/c. It is well-known that the signal to noise ratio of the particle deflections in a magnet plug varies as $\sqrt{z}$ where z is the thickness of the plug (e.g. O'Connor and Wolfendale, 1960). Thus,

bigger plugs ($z > 45$ cm) would be more practical. The
method of detecting the badly scattered particles by a
suitable check measurement (section 4.2.2.) also offers
practical possibilities.

In the present work the theoretical scattering correc-
tion method had to be used (section 4.2). It was found that
in more general terms the correction was a statistical analy-
sis of an indirect determination of an unknown distribution
function. Insufficient attention seems to have been devoted
previously to the theory of such analysis. In practical
applications there are normally some general theorectical
requirements which can be attributed to the unknown function;
one requirement usually concerns the smoothness. According
to the example given in section 4.2.9, the requirements on
smoothness, or on some expected curvature, can be incorporated
in a fitting calculation by adding to the expression for χ^2
a quantity ω^2 corresponding to the extra requirements.

From what has been said it is clear that, despite the
difficulties caused by phenomena such as Coulomb scattering,
muon studies are still a source of useful information about
high-energy nuclear interactions. With the development of
bigger and more sophisticated spectrographs further improve-
ments in knowledge are expected.

ACKNOWLEDGMENTS

The author wishes to thank Professor G. D. Rochester, F.R.S., for the provision of the facilities for this work and also for his continuous support and interest.

It is with gratitude that the author acknowledges the guidance and encouragement of his supervisor, Professor A. W. Wolfendale, in this work.

The author is indebted to Professor Väinö Hovi, University of Turku, Finland, for his unfailing support.

The work of Mr. K. Gijsbers and Professor Y. Kamiya during the preparation of the present experiment is acknowledged with thanks. Drs. G. Brooke and K. M. Pathak are thanked for their help in the experiment and for valuable discussions.

The technical staff of the Physics Department, in particular Mr. W. Threadgill, Mr. E. Lincoln, Mr. K. Tindale, Miss C. Guyll, and Miss P. Wallace are thanked for their willing help.

Warm thanks are due to the author's wife, Mrs. M. A. Aurela, for her help in the preparation of this thesis, to Dr. I. W. Rogers for his careful work in checking the manuscript, and to Mrs. M. E. Leggett for its typing.

The author had a scholarship from the British Council in 1963 - 1964, a studentship from the University of Turku in 1963, a studentship from Väinö Edvard Miettisen Stipendirahasto,

APPENDIX 1

ELECTRONIC CIRCUITS

This appendix contains the circuit diagrams of the units which were considerably changed after Palmer's work (1964).

Fig. Al.1 shows the improved design of the quenching unit. In the coincidence unit (Fig. Al.2) the output circuitry was modified. In the momentum selector (Fig. Al.3) the working conditions of some valves were made more stable and an amplifier valve was added. The control unit (Fig. Al.4) was changed to a mechanical switch system driven by a motor.
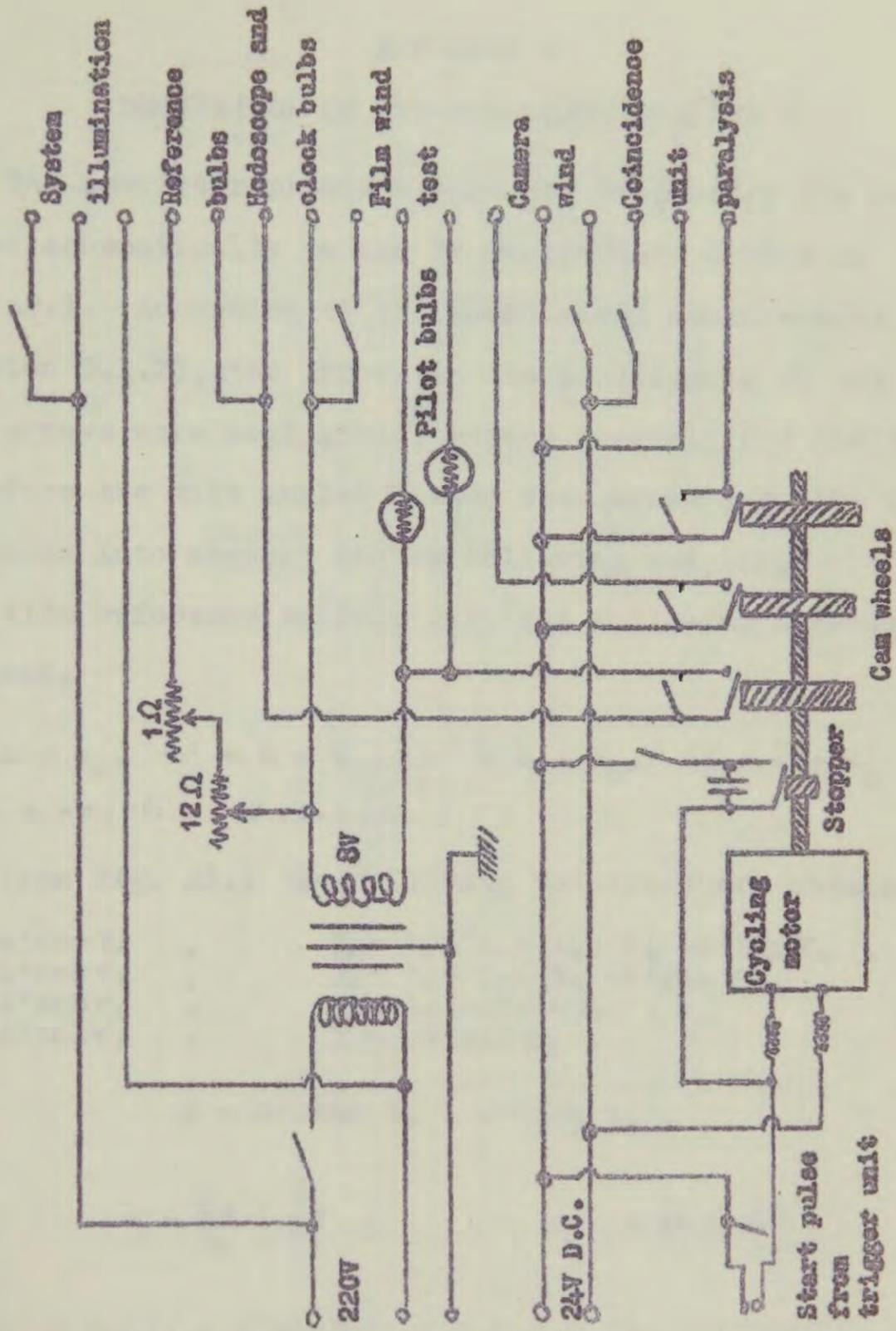
Fig. A1.1 The quenching unit for Geiger counters.

Fig. A1.2 The coincidence unit.

Fig. A1.3 The momentum selector.

Fig. A1.4 The control unit.

APPENDIX 2

DERIVATION OF THE FORMULAE FOR Δ AND x

The spectrograph and a particle trajectory are represented schematically in the XY co-ordinate system in Fig. A2.1. According to the geometrical measurements (section 3.1.2), the errors in the positioning of the flash tube arrays were negligible, except possibly for the tilt. Therefore the tilt angles τ have been drawn into the figure and taken into account in the following analysis.

With reference to Fig. 2.4, the following abbreviations are used:

$$a' = a + a_0, \quad b' = b + b_0, \quad c' = c + c_0, \quad d' = d + d_0 \qquad A2.1$$

$(a_0 < 0, \ b_0 < 0, \ etc., \ a > 0, \ b > 0, \ etc.)$.

Then from Fig. A3.1 the following relations are obtained:

$$\begin{aligned}
X_A &= -a'\cos\tau_A \quad, & Y_A &= l_1 + l_2 + l_3 + l_4 - a'\sin\tau_A \quad, \\
X_B &= -b'\cos\tau_B \quad, & Y_B &= l_2 + l_3 + l_4 - b'\sin\tau_B \quad, \\
X_C &= -c'\cos\tau_C \quad, & Y_C &= l_4 - c'\sin\tau_C \quad, \\
X_D &= -d'\cos\tau_D \quad, & Y_D &= -d'\sin\tau_D \quad,
\end{aligned} \qquad A2.2$$

$$\phi = \arctan t_4 - \arctan t_1 \quad, \qquad A2.3$$

$$t_1 = \frac{X_A - X_B}{Y_A - Y_B} \quad, \qquad t_4 = \frac{X_C - X_D}{Y_C - Y_D} \quad, \qquad A2.4$$

$$X_1 = X_B - t_1(l_2 - b'\sin\tau_B), \quad X_2 = X_C + t_4(l_3 + c'\sin\tau_C). \qquad A2.5$$

Flash-tube
arrays

+Y

Particle trajectory

North

A

South

a'

τ_A

X_A, Y_A

l_1

X_B, Y_B

B

τ_B

b'

Magnet
plug

l_2

X_1 X_2

ϕ

l_3

X_C, Y_C c'
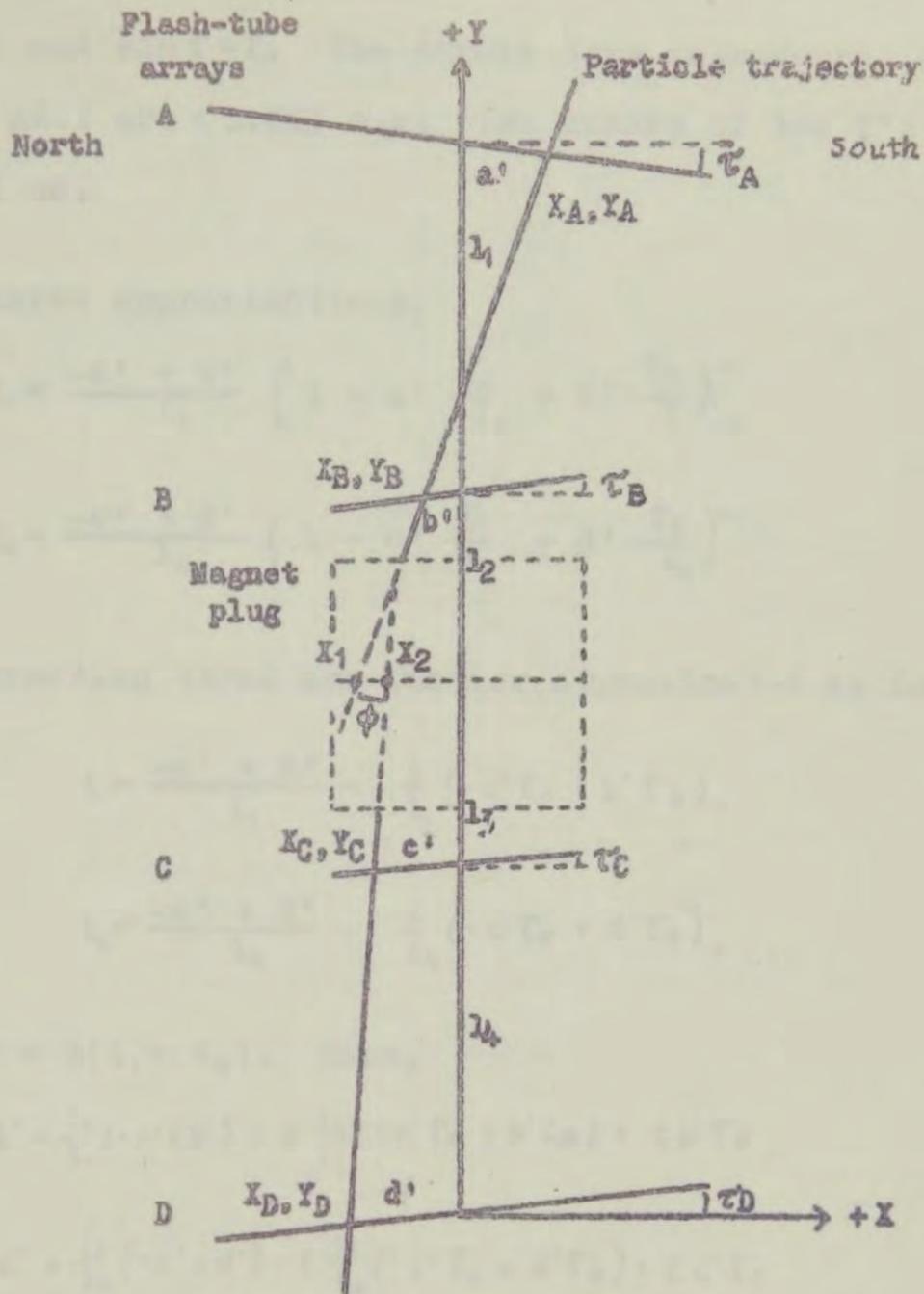
C

τ_C

l_4

X_D, Y_D d'

D

τ_D

+X

Fig. A2.1 The geometry for the determination
of a particle trajectory.

The equations A2.2 and A2.5 are approximated by setting $\cos\tau \approx 1$ and $\sin\tau \approx \tau$. The errors thus introduced into the X's in A2.2 are < 0.003 t.s. The errors of the Y's are < 0.00001 cm.

After these approximations,

$$t_1 = \frac{-a' + b'}{l_1}\left(1 - a'\frac{\tau_A}{l_1} + b'\frac{\tau_B}{l_1}\right)^{-1},$$

$$t_4 = \frac{-c' + d'}{l_4}\left(1 - c'\frac{\tau_C}{l_4} + d'\frac{\tau_D}{l_4}\right)^{-1}.$$

The correction terms are further approximated as follows:

$$t_1 = \frac{-a' + b'}{l_1} - \frac{t}{l_1}(-a'\tau_A + b'\tau_B),$$

$$t_4 = \frac{-c' + d'}{l_4} - \frac{t}{l_4}(-c'\tau_C + d'\tau_D),$$

A2.6

where $t = \frac{1}{2}(t_1 + t_4)$. Then,

$$X_1 = -b' - \frac{l_2}{l_1}(-a'+b') + t\frac{l_2}{l_1}(-a'\tau_A + b'\tau_B) + t b'\tau_B,$$

$$X_2 = -c' + \frac{l_3}{l_4}(-c'+d') - t\frac{l_3}{l_4}(-c'\tau_C + d'\tau_D) + t c'\tau_C.$$

A2.7

The equation A2.3 is approximated as follows:

$$\emptyset \approx t_4 - t_1 - \frac{1}{3}(t_4^3 - t_1^3).$$

The corresponding error in $\emptyset$ is $< 10^{-5}$ rad. The correction term is approximated further:

$$-\tfrac{1}{3}(t_4^3 - t_1^3) = -\tfrac{1}{3}(t_4 - t_1)(t_4^2 + t_4 t_1 + t_1^2) \approx -\emptyset t^2.$$

Thus,

$$\emptyset = t_4 - t_1 - \emptyset t^2. \qquad\qquad A2.8$$

Accurately, Δ is to be defined as follows:

$$\Delta = l_1 \emptyset . \qquad\qquad A2.9$$

The following approximation is now studied:

$$\Delta' = a' - b' + \frac{l_1'}{l_4}(-c' + d') .$$

According to A2.6, A2.8, and A2.9,

$$\Delta = \Delta' + tT_1 - t^2 \Delta' \qquad\qquad A2.10$$

where the tilt correction T_1 is

$$T_1 = -a'\tau_A + b'\tau_B + c'\tau_C - d'\tau_D.$$

The further approximated quantity

$$\Delta'' = a' - b' - c' + d' \qquad\qquad (2.2a)$$

which is used in equation 2.2 is related to Δ' by the equation:

$$\Delta' = \Delta'' + t(l_1 - l_4). \qquad\qquad A2.11$$

The discrepancy at the centre of the magnetic field is defined as

$$x = X_2 - X_1 \qquad\qquad A2.12$$

(see Hayman and Wolfendale, 1962). A useful approximation

to x is:

$$x' = -\frac{l_2}{l_1} a' + (1 + \frac{l_2}{l_1})b' - (1 + \frac{l_3}{l_4})c' + \frac{l_3}{l_4}d' . \qquad A2.13$$

According to A2.7

$$x = x' + tT_2 \qquad\qquad A2.14$$

where

$$T_2 = \frac{l_2}{l_1} a'\tau_A - (1 + \frac{l_2}{l_1}) b'\tau_B + (1 + \frac{l_3}{l_4}) c'\tau_C - \frac{l_3}{l_4} d'\tau_D .$$

In order to get an idea of the magnitude of the errors caused by neglecting the correction terms the corresponding standard deviations in Δ are estimated. For the "inclination error", $t(l_1 - l_4)$, $\sigma_\Delta \approx 0.04$ t.s. For the "deflection error", $t^2\Delta'$, $\sigma_\Delta \approx 0.08$ t.s. For the tilt error, $-tT_1$, $\sigma_\Delta \approx$ 0.03 t.s. The largest possible error is due to the deflection error and is 0.3 t.s. However, this is not possible for high-energy particles with $\Delta \leq 1$ t.s. The total effect of these errors was calculated for 89 events with $\Delta < 1.2$ t.s. In two cases only was the total error > 0.1 t.s. Thus the errors made in the geometrical approximations are insignificant and the use of the simplified equations 2.2 and A2.13 is justified.

APPENDIX 3

CALCULATION OF THE ACCEPTANCE FUNCTION A(Δ)

Brooke et al. (1962) integrated the acceptance function of the original spectrograph. As the detector system has since been changed, e.g. the 'gap counters' were removed, a somewhat different integration is needed here, as shown below.

The integration of the function A(Δ) (section 4.1.2) is performed in the middle plane of the spectrograph (Fig. A3.1). Because the counter trays are rectangular and because their dimensions are small compared with L_1 and L_2, the integration may be carried out separately in the north-south plane and in the east-west plane as follows:

$$A(\phi) = A_1(\phi)A_2. \qquad \qquad \text{A3.1}$$

In the north-south plane, the acceptance angle Y is integrated along the axis X:

$$A_1 = \int Y \, dX. \qquad \qquad \text{A3.2}$$

For X near the vertical axis of the spectrograph, Y is defined by the trays A and D, and is given by the triangle (1) in Fig. A3.1. Further away from the vertical axis, Y is defined by the trays B and C as shown by the triangle (2). The common area of the triangles is equal to $A_1(\phi)$.

For a deflection ϕ the triangles are displaced by $+(L_1 + L_2)\phi$ and $+\frac{1}{2}L_2\phi$ from the origin, respectively. For the
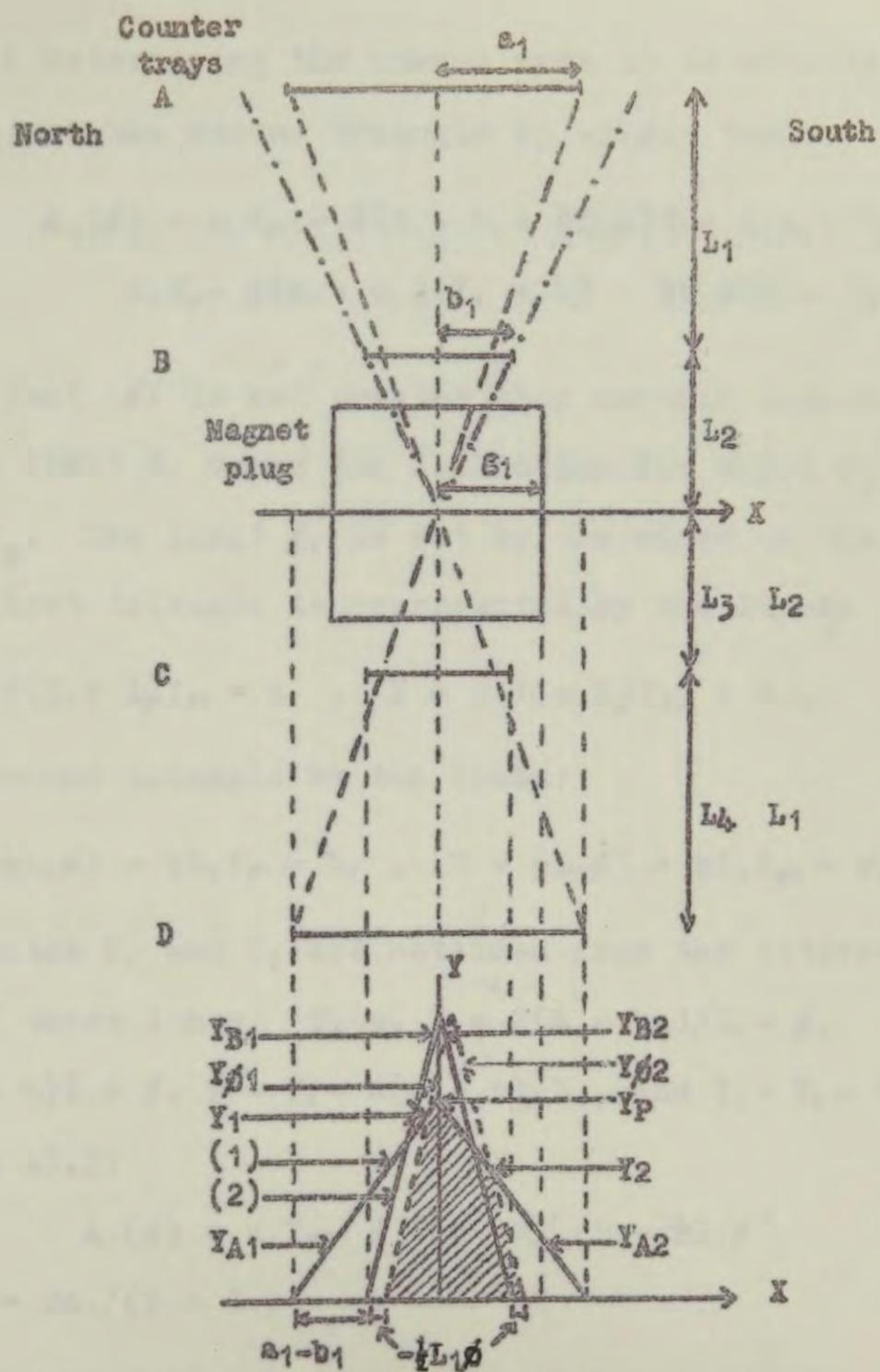
Fig. A3.1 The acceptance geometry
of the spectrograph.

purpose of determining the common area it is sufficient to displace just the second triangle by $-L_1\phi$. Thus,

$$A_1(\phi) = a_1 Y_P - \tfrac{1}{2}(a_1 - b_1 + \tfrac{1}{2}L_1\phi)Y_1 - \tfrac{1}{2}(a_1 - b_1 - \tfrac{1}{2}L_1\phi)Y_2 =$$
$$a_1 Y_P - \tfrac{1}{2}(a_1 - b_1)(Y_1 + Y_2) - \tfrac{1}{4}L_1\phi(Y_1 - Y_2), \qquad \text{A3.3}$$

provided that $|\phi|$ is not greater than certain limits ϕ_1 and ϕ_2. The limit ϕ_1 means the deflection for which Y_1 or Y_2 becomes Y_p. The limit ϕ_2 is set by the edges of the plug.

The first triangle is represented by the lines:

$$-X + \tfrac{1}{2}(L_1 + L_2)Y_{A1} = a_1 \quad , \quad X + \tfrac{1}{2}(L_1 + L_2)Y_{A2} = a_1, \qquad \text{A3.4}$$

and the second triangle by the lines:

$$-(X + \tfrac{1}{2}L_1\phi) + \tfrac{1}{2}L_2 Y_{\phi 1} = b_1 \quad , \quad (X + \tfrac{1}{2}L_1\phi) + \tfrac{1}{2}L_2 Y_{\phi 2} = b_1. \qquad \text{A3.5}$$

The ordinates Y_1 and Y_2 are obtained from the intersection points of these lines. Thus, $Y_1 = 2(a_1 - b_1)/L_1 - \phi$, $Y_2 = 2(a_1 - b_1)L_1 + \phi$, $Y_1 + Y_2 = 4(a_1 - b_1)/L_1$, and $Y_1 - Y_2 = 2\phi$. Then from A3.3:

$$A_1(\phi) = a_1 Y_P - 2(a_1 - b_1)^2/L_1 - \tfrac{1}{2}L_1\phi^2 \qquad \text{A3.6}$$

where $Y_P = 2a_1/(L_1 + L_2)$.

The limit ϕ_1 is obtained from A3.5 by setting $X = 0$ and $Y = Y_P$. Thus,

$$\phi_1 = (2b_1 - L_2 Y_P)/L_1. \qquad \text{A3.7}$$

The other limit is not got from Fig. A3.1:

$$\phi_2 = (2g_1 - 2b_1)/L_2. \qquad \text{A3.8}$$

The function A_2 is obtained in a similar way. It is
only interesting from the point of view of the absolute
value of the collecting power of the spectrograph. For
this purpose, the scattering may be neglected and then
$\phi_{EW} = 0$.

Thus,

$$A_2 = 2a_2{}^2/(L_1 + L_2) - 2(a_2 - b_2)^2/L_1. \qquad A3.9$$

APPENDIX 4

CALCULATION OF THE BIAS FUNCTION B (Δ)

In order to work out the function $B(\Delta)$ in equation 4.1, the results of Palmer (1964) on the relative frequency of the accompanied muons should be converted to refer to the differential spectra. To facilitate the conversion, the experimental results will be represented by an analytical expression which, at the same time, may be expected to smooth out part of the statistical fluctuation. It is found that the experimental points are a good fit to the following power law:

$$r(\Delta) = I_a(\Delta)/I_s(\Delta) = 0.20\,\Delta^{-0.10} \quad (\Delta \text{ in t.s.}) \qquad \text{A4.1}$$

where I_a and I_s are the integral scattered spectra for accompanied and single muons, respectively. It should be remembered, however, that the statistical errors are large (see Fig. A4.1).

The integral spectrum of all muons is

$$I(\Delta) = I_s + I_a = I_s[1 + r] \ .$$

Thus, the corresponding differential spectra are related by equation:

$$i(\Delta) = i_s[1 + r] + I_s\,(dr/d\Delta)$$

where $dr/d\Delta = -0.10\,r/\Delta$ according to equation A4.1. Then,

$$z(\Delta) = 1_a / 1 = 1 / [1 + \sigma_s + \sigma_c(\Delta) 1 - \sigma_s / \sigma_c]$$

The quantities σ_s and $\sigma_c(\Delta)$ which enter into ...

The values of $z(\Delta)$ ...

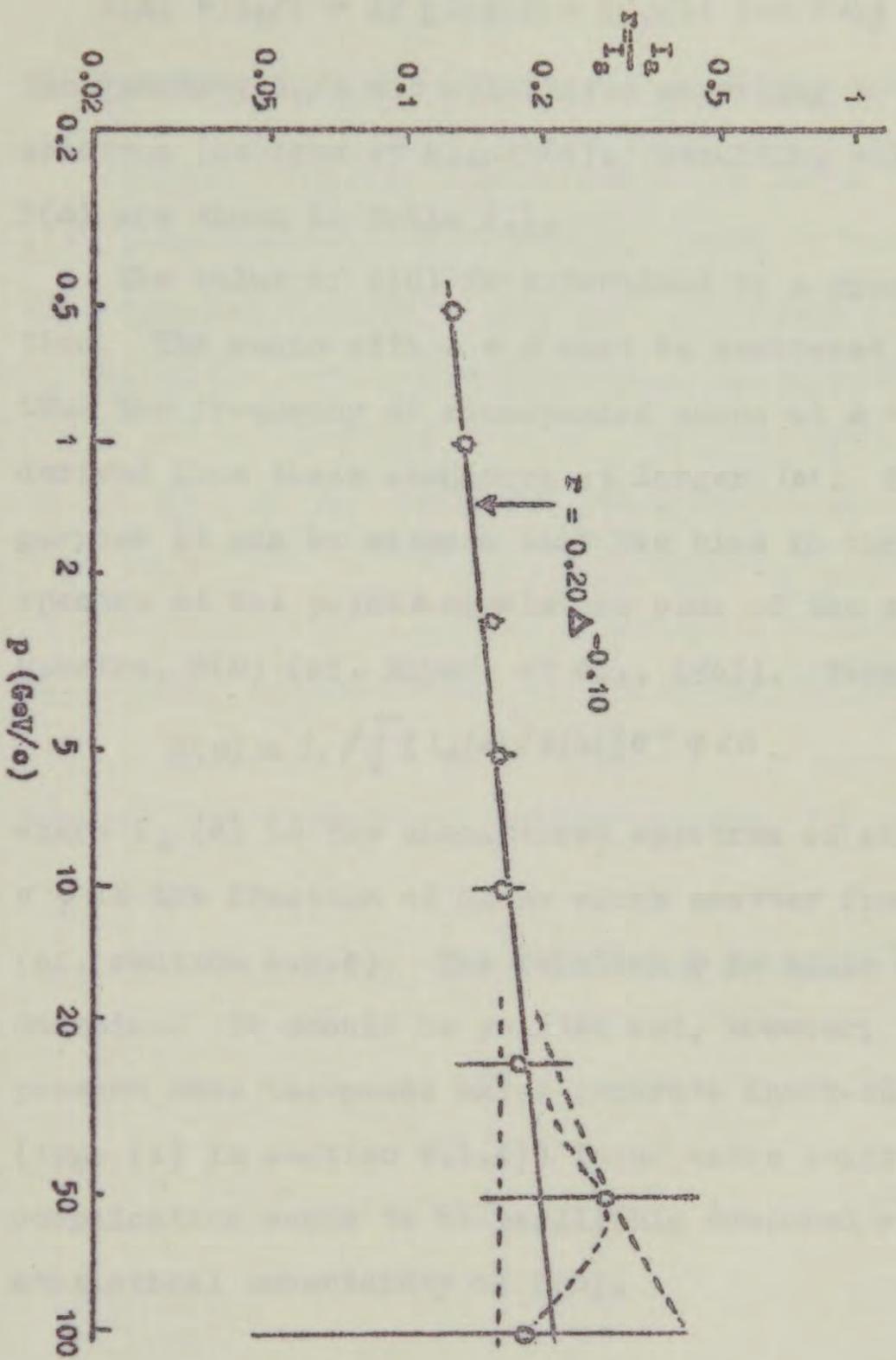$$z(\Delta) = 1_a / \int_1^\infty L(\Delta, z) \, \text{sin}(z)^x \, d\sigma$$

Fig. 14.1 The ratio between the integral spectrum of accompanied muons, I_a, and the integral spectrum of single muons, I_s; the experimental points are from Palmer (1964).

$\dfrac{I_a}{I_s}$

p = 0.20 Δ^{-0.10}

p (GeV/c)

$$B(\Delta) = i_s/i = 1/\left[1 + r + (I_s/i)(dr/d\Delta)\right] \quad . \qquad A4.2$$

The quantity I_s/i was calculated according to the OWP spectrum (Osborne et al., 1964). Resulting values of $B(\Delta)$ are shown in table 4.1.

The value of $B(0)$ is determined by a special calculation. The muons with $\Delta = 0$ must be scattered muons and thus the frequency of accompanied muons at $\Delta = 0$ can be derived from their abundance at larger $|\Delta|$. For this purpose it can be assumed that the bias in the unscattered spectra at the point Δ equals the bias of the scattered spectra, $B(\Delta)$ (cf. Hayman et al., 1963). Then,

$$B(0) \approx i_s \bigg/ \int_o^\infty \left[i_u(\Delta)/B(\Delta)\right]\sigma^{-1}\varphi\, d\Delta . \qquad A4.3$$

where $i_u(\Delta)$ is the unscattered spectrum of all muons and $\sigma^{-1}\varphi$ is the fraction of muons which scatter from Δ to 0 (cf. section 4.2.4). The function φ is again assumed to be Gaussian. It should be pointed out, however, that in the present case the muons which generate knock-on electrons (type (i) in section 4.1.4)) incur extra scattering. This complication seems to be negligible compared with the large statistical uncertainty of $B(\Delta)$.

APPENDIX 5

THE MAGNETIC DISPLACEMENT AND SCATTERING DISPLACEMENT
OF A PARTICLE UNDERGOING ENERGY LOSS

Ashton and Wolfendale (1964) have worked out the relationship between the momentum of a muon and its displacement in a spectrograph with a solid iron magnet taking into account the energy loss. In the present experiment, the effect of the energy loss is significant in the range $4 < \Delta < 8.15$ t.s. and in the calculation of the scattering from the range $\Delta > 8.15$ t.s. the effect becomes increasingly important. The theory is therefore briefly presented here.

Fig. A5.1 shows the trajectory of a muon, momentum p_1, incident on a block of magnetized iron at a small angle θ_1 with the normal to the surface and the plane perpendicular to the lines of magnetic flux. The magnetic induction is denoted by B and the mean momentum loss per unit path length in the iron by α (assumed constant over the trajectory). The equation of the trajectory is

$$p_1 - \alpha \int_0^X [1 + (dy/dx)^2]^{1/2} dx = 300 B [1 + (dy/dx)^2]^{3/2} (d^2y/dx^2)^{-1}.$$

In the present spectrograph, the angles with the normal are small and the solution for the angular deflection at the point of emergence from the magnet is

$$\phi = \theta_2 - \theta_1 = -300 \frac{B}{\alpha} \ln\left(1 - \frac{\alpha l_1}{p_1}\right).$$

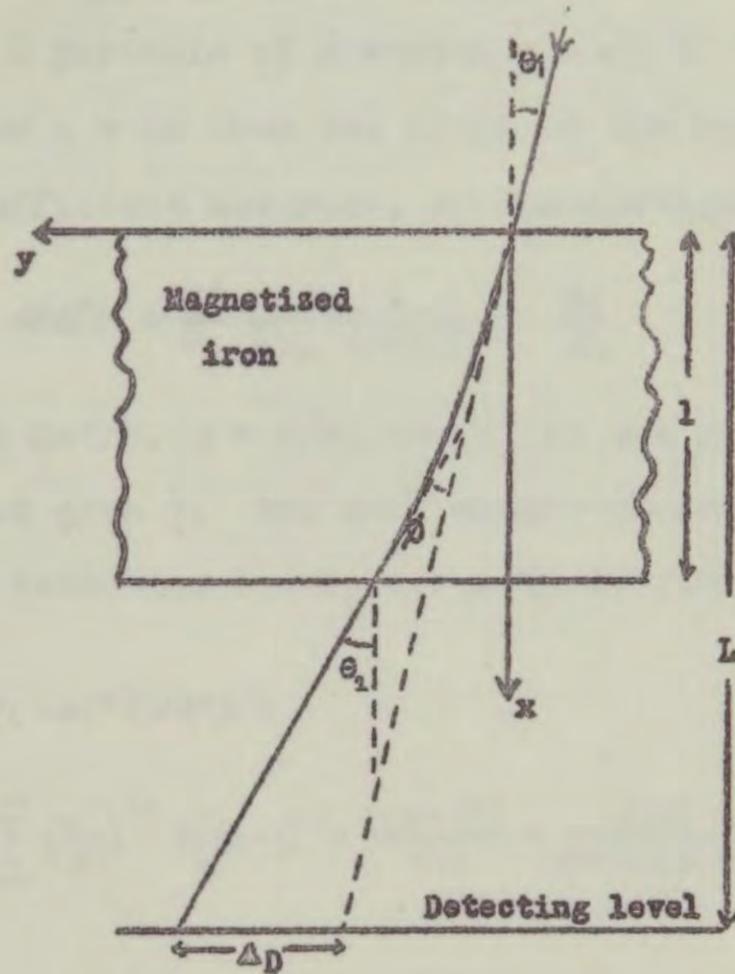$$(\gamma^2) = \int_0^L (\gamma) \, d\gamma$$

Fig. A5.1 The trajectory of a muon in
a block of magnetised iron.

The displacement measured in the present experiment is

$\Delta = (\theta_2 - \theta_1)l_1$ (section 2.6).

The mean square projected angle of scatter $\langle d\theta^2 \rangle$ suffered by a particle of momentum $p_1 - \alpha x$ in travelling between x and $x + dx$ from the front of the magnet is given, to sufficient accuracy, by the equation

$$\langle d\theta^2 \rangle = \frac{K^2}{2} \frac{1}{(p_1 - \alpha x)^2 \beta^2} \frac{dx}{X_0}$$

where $K = 21$ MeV/c, $\beta = v/c$, and X_0 is the radiation length in iron (13.8 g/cm). The mean square projected displacement $\langle y^2 \rangle$ at the detection level, for $\beta \rightarrow 1$, is given by

$$\langle y^2 \rangle = \int_0^1 (L-x)^2 \langle d\theta^2 \rangle =$$

$$\frac{K^2}{2 X_0 p_1^2} \sum_{n=1}^{\infty} \left(\frac{\alpha l}{p_1}\right)^{n-1} l\left\{(L-1)^2 + \frac{2(L-1)l}{n+1} + \frac{2 l^2}{(n+1)(n+2)}\right\}. \qquad A5.2$$

REFERENCES

Ashton, F., Kamiya, Y., MacKeown, P. K., Osborne, J. L.,
        Pattison, J. B. M., Ramana Murthy, P. V., and
        Wolfendale, A. W., 1965, Proc. Phys., Soc.,
        in the press.

Ashton, F., MacKeown, P. K., Pattison, J. B. M., and
        Wolfendale, A. W., 1964, Cosmic Ray Sea Level
        Muon Interactions, Final Technical Report,
        Grant No. AF EOAR 62-117, USAF Cambridge
        Research Laboratory.

Ashton, F., MacKeown, K., Ramana Murthy, P. V., Pattison,
        J. B. M., and Wolfendale, A. W., 1965, Physics
        Letters, 6, 259.

Ashton, F., and Wolfendale, A. W., 1963, Proc. Phys. Soc.,
        81, 593.

Babayan, Kh. P., Brikker, S.I., Grigorov, N. L., Podgurskaya,
        A. V., Savelyeva, A. I., and Shestoperov, V. Ya.,
        1963, Proc. Int. Conf. on Cosmic Rays, Jaipur,
        India, 5, 51 (Bombay: Commercial Printing Press).

Bowler, M. G., Fowler, P. H., and Perkins, D. H., 1962,
        Nuovo Cim., 26, 1182.

Brooke, G., 1964, Ph.D. Thesis, University of Durham.

Brooke, G., Gardener, M., Lloyd, J. L., Kisdnasamy, S., and
        Wolfendale, A. W., 1962, Proc. Phys. Soc., 80, 674.

Brooke, G., Hayman, P. J., Kamiya, Y., and Wolfendale, A. W.,
1964, Proc. Phys., Soc., 83, 853.

Cocconi, G., 1958, Phys. Rev. III, 1699.

Cocconi, G., 1965, Proc. Int. Conf. on Cosmic Rays, London,
(The Institute of Physics and The Physical
Society), to be published.

Cocconi, G., Koester, L. J., and Perkins, D. H., 1961,
Lawrence Radiation Laboratory Report, High
Energy Study Seminars, No. 28, Part 2.

Coxell, H., and Wolfendale, A. W., 1960, Proc. Phys. Soc.,
35, 378.

Cramér, H., 1946, Mathematical Methods of Statistics
(Princeton: University Press).

Crossland, A. D., and Fowler, G. N., 1965, Proc. Int. Conf.
on Cosmic Rays, London (The Institute of Physics
and The Physical Society), to be published.

Dmitriev, V. A., and Khristiansen, G. B., 1963, J. Exptl.
Theoret. Phys. (U.S.S.R.), 44, 405, Soviet
Physics JETP, 17, 276.

Dodd, P., Jobes, L., Kinson, J., Tallini, B., French, B.R.,
Sherman, H. J., Skillicorn, I. O., Davies, W. T.,
Derrick, M., and Radojicic, D., 1961, Int. Conf.
on Elementary Particles, Aix-en-Provence, 1, 433
(Saclay: C.E.N.).

Duthie, J., Fowler, P. H., Kaddoura, A., Perkins, D. H.,
and Pinkau, K., 1962, Nuovo Cim., 24, 122.

Feinberg, E. L., 1965, Proc. Int. Conf. on Cosmic Rays,
        London (The Institute of Physics and The
        Physical Society), to be published.

Fowler, G. N., and Wolfendale, A. W., 1961, Handbuch d.
        Phys., $\underline{46/1}$, 272 (Berlin: Springer).

Gardener, M., Jones, D. G., Taylor, F. E., and Wolfendale,
        A. W., 1962, Proc. Phys. Soc., $\underline{80}$, 697.

Gell-Mann, M., 1964, Phys. Letters, $\underline{8}$, 214.

Grigorov, N. L., Kotov, Yu. D., and Rosental, I. L., 1963,
        Proc. Int. Conf. on Cosmic Rays, Jaipur, India,
        $\underline{5}$, 265 (Bombay: Commercial Printing Press).

Grigorov, N. L., Nesterov, V. E., Rapoport, I. D.,
        Savenko, I. A., and Skuridin, G. A., 1965,
        Proc. Int. Conf. on Cosmic Rays, London (The
        Institute of Physics and The Physical Society),
        to be published.

Grigorov, N. L., and Shestoperov, V. Ya., 1963, Proc. Int.
        Conf. on Cosmic Rays, Jaipur, India, $\underline{5}$, 268
        (Bombay: Commercial Printing Press).

Guseva, V. V., Dobrotin, N. A., Zelevinskaya, N. G.,
        Kotelnikov, K. A., Lebedev, A. M., and
        Slavatinsky, S. A., 1962, Proc. Int. Conf. on
        Cosmic Rays and the Earth Storm, Kyoto, 1961
        (J. Phys. Soc. Japan (Suppl. AIII), $\underline{17}$, 375)).

Hartree, D. R., 1964, Numerical Analysis, 2nd edition
(London: Oxford University Press).

Hayman, P. J., 1962, Ph.D. Thesis, University of Durham.

Hayman, P. J., Palmer, N. S., and Wolfendale, A. W., 1963,
Proc. Phys. Soc. A, 275, 391.

Hayman, P. J., and Wolfendale, A. W., 1962, Proc. Phys.
Soc., 80, 710.

Higashi, S., Kitamura, T., Watase, Y., Oda, M., Tanaka, Y.,
1964, Nuovo Cim., 32, 1.

Holmes, J. E. R., Owen, B.G., and Rodgers, A. L., 1961,
Proc. Phys. Soc., 78, 505.

Hovi, V., and Aurela, A., 1961, Ann. Acad. Sci. Fenn. A VI,
No. 97.

Japanese Emulsion Group and Brazilian Emulsion Group, 1963,
Proc. Int. Conf. on Cosmic Rays, Jaipur, India,
5, 326 (Bombay: Commercial Printing Press).

Jones, D. G., 1961, Ph.D. Thesis, University of Durham.

Jones, D. G., Taylor, F. E., and Wolfendale, A. W., 1962,
Proc. Phys. Soc., 80, 686.

Kitamura, T., and Takahashi, T., 1963, Proc. Int. Conf. on
Cosmic Rays, Jaipur, India, 6, 229 (Bombay:
Commercial Printing Press).

Koba, Z., 1965, Proc. Int. Conf. on Cosmic Rays, London
(The Institute of Physics and The Physical
Society), to be published.

Kopal, Z., 1961, Numerical Analysis (London: Chapman & Hall).

Krasilnikov, D. D., 1963, Proc. Int. Conf., on Cosmic Rays, Jaipur, India, 6, 124 (Bombay: Commercial Printing Press).

MacKeown, P. K., Pattison, J. B. M., Ramana Murthy, P. V., and Wolfendale, A. W., 1963, Proc. Int. Conf. on Cosmic Rays, Jaipur, India, 6, 41 (Bombay: Commercial Printing Press).

MacKeown, P. K., Said, S. S., Wdowczyk, J., and Wolfendale, A. W., 1965 a, Proc. Int. Conf. on Cosmic Rays, London, paper MU-NU 3, (The Institute of Physics and The Physical Society), to be published.

MacKeown, P. K., Said, S. S., Wdowczyk, J., and Wolfendale, A. W., 1965 b, Proc. Int. Conf. on Cosmic Rays, London, paper MU-NU 14, (The Institute of Physics and The Physical Society), to be published.

Malholtra, P. K., Shukla, P. G., Stephens, S. A., Vijayalakshmi, B., Boult, J., Bowler, M. G., Clapham, V. M., Fowler, P. H., Hackforth, H. L., Keereetaveep, J., and Tovey, S. N., 1965, Proc. Int. Conf. on Cosmic Rays, London, (The Institute of Physics and The Physical Society), to be published.

Miyake, S., Narasimham, V. S., and Ramana Murthy, P. V., 1964, Nuovo Cim., _32_, 1524.

Narayan, D. S., 1964, Nuovo Cimento _34_, 981.

O'Connor, P. V., and Wolfendale, 1960, Suppl, Nuovo Cim. _15_, No. 2, 202.

Osborne, J. L., and Wolfendale, A. W., 1964, Proc. Phys. Soc., _84_, 901.

Osborne, J. L., Wolfendale, A. W., and Palmer, N. S., 1964, Proc. Phys. Soc., _84_, 911.

Palmer, N. S., 1964, M.Sc. Thesis, University of Durham.

Peters, B., 1963, Proc. Int. Conf. on Cosmic Rays, Jaipur, India, _5_, 423 (Bombay: Commercial Printing Press).

Peters, B., 1965, Proc. Int. Conf. on Cosmic Rays, London (The Institute of Physics and The Physical Society), to be published.

Ramana Murthy, P. V., 1963, Proc. Int. Conf. on Cosmic Rays, Jaipur, India, _6_, 22 (Bombay: Commercial Printing Press).

Rastin, B. C., Baber, S. R., Bull, R. M., and Nash, W. F., 1965, Proc. Int. Conf. on Cosmic Rays, London (The Institute of Physics and The Physical Society), to be published.

Rochester, G. D., 1963, Proc. Int. Conf. on Cosmic Rays, Jaipur, India, _6_, 237 (Bombay: Commercial Printing Press).

Rochester, G. D., Somogyi, A. J., Turver, K. E., and
　　　　Walton, A. B., 1965, Proc. Int. Conf. on
　　　　Cosmic Rays, London, (The Institute of Physics
　　　　and the Physical Society), to be published.

Rossi, B., 1948, Rev. Mod. Phys., 20, 537.

Rossi, B., 1961, High Energy Particles (Englewood Cliffs,
　　　　N. J.: (Prentice-Hall).

Scarborough, J. B., 1950, Numerical Mathematical Analysis
　　　　(London: Oxford University Press).

Vernov, S. N., 1965, Proc. Int. Conf. in Cosmic Rays,
　　　　London, (The Institute of Physics and The
　　　　Physical Society), to be published.

Vernov, S. N., Khristiansen, G. B., Netchin, Ju. A.,
　　　　Vedenev, O. V., Khrenov, B. A., 1965, Proc.
　　　　Int. Conf. on Cosmic Rays, London, (The
　　　　Institute of Physics and The Physical Society),
　　　　to be published.

Wolfendale, A. W., 1963, Proc. Int. Conf. on Cosmic Rays,
　　　　Jaipur, India, 6, 3 (Bombay: Commercial Printing
　　　　Press).

Wolfendale, A. W., 1965, Proc. Int. Conf. on Cosmic Rays,
　　　　London, (The Institute of Physics and The
　　　　Physical Society), to be published.

Yash Pal, 1963, Proc. Int. Conf. on Cosmic Rays, Jaipur,
　　　　India, 5, 445 (Bombay: Commercial Printing Press).